

Switch-like and persistent memory formation in individual *Drosophila* larvae

Amanda Lesar¹, Javan Tahir¹, Jason Wolk¹, Marc Gershow^{1,2,3*}

¹Department of Physics, New York University, New York, United States; ²Center for Neural Science, New York University, New York, United States; ³NYU Neuroscience Institute, New York University Langone Medical Center, New York, United States

Abstract Associative learning allows animals to use past experience to predict future events. The circuits underlying memory formation support immediate and sustained changes in function, often in response to a single example. Larval *Drosophila* is a genetic model for memory formation that can be accessed at molecular, synaptic, cellular, and circuit levels, often simultaneously, but existing behavioral assays for larval learning and memory do not address individual animals, and it has been difficult to form long-lasting memories, especially those requiring synaptic reorganization. We demonstrate a new assay for learning and memory capable of tracking the changing preferences of individual larvae. We use this assay to explore how activation of a pair of reward neurons changes the response to the innately aversive gas carbon dioxide (CO₂). We confirm that when coupled to CO₂ presentation in appropriate temporal sequence, optogenetic reward reduces avoidance of CO₂. We find that learning is switch-like: all-or-none and quantized in two states. Memories can be extinguished by repeated unrewarded exposure to CO₂ but are stabilized against extinction by repeated training or overnight consolidation. Finally, we demonstrate long-lasting protein synthesis dependent and independent memory formation.

Introduction

Associative learning allows animals to use past experience to predict important future events, such as the appearance of food or predators, or changes in their environmental conditions (Pavlov, 1927; Kandel et al., 2014). The *Drosophila* larva is a favorable model system for the study of learning and memory formation (Gerber et al., 2013; Widmann et al., 2018; Quinn and Dudai, 1976; Scherer et al., 2003; Apostolopoulou et al., 2013; Neuser et al., 2005; Saumweber et al., 2018), with approximately 10,000 neurons in its representative insect brain. Widely available experimental tools allow manipulation of gene expression and introduction of foreign transgenes in labeled neurons throughout the *Drosophila* brain, including in the learning and memory centers (Saumweber et al., 2018; Eichler et al., 2017; Li et al., 2014; Duffy, 2002), whose synaptic connectivities can be reconstructed via electron microscopy (Eichler et al., 2017; Eschbach et al., 2020a; Eschbach et al., 2020b).

Larvae carry out complex behaviors including sensory-guided navigation (Luo et al., 2010; Klein et al., 2015; Fishilevich et al., 2005; Asahina et al., 2009; Gomez-Marin and Louis, 2014; Gershow et al., 2012; Gomez-Marin et al., 2011; Sawin et al., 1994; Kane et al., 2013; Busto et al., 1999; Humberg et al., 2018), which can be modified by learning (Gerber et al., 2013; Scherer et al., 2003; Neuser et al., 2005; Widmann et al., 2018). Larval *Drosophila* has long been a model for the study of memory formation, with a well-established paradigm developed to study associative memory formation through classical conditioning (Gerber et al., 2013; Widmann et al., 2018; Schleyer et al., 2018; Scherer et al., 2003; Neuser et al., 2005; Gerber and Stocker, 2007; Apostolopoulou et al., 2013; Saumweber et al., 2018; Weiglein et al., 2019). In this paradigm, larvae are trained and tested in groups, and learning is quantified by the difference in the olfactory

*For correspondence:
mhg4@nyu.edu

Competing interests: The authors declare that no competing interests exist.

Funding: See page 26

Preprinted: 15 April 2021

Received: 13 May 2021

Accepted: 27 August 2021

Published: 12 October 2021

Reviewing editor: Gordon J Berman, Emory University, United States

© Copyright Lesar et al. This article is distributed under the terms of the [Creative Commons Attribution License](https://creativecommons.org/licenses/by/4.0/), which permits unrestricted use and redistribution provided that the original author and source are credited.

eLife digest Brains learn from experience. They take events from the past, link them together, and use them to predict the future. This is true for fruit flies, *Drosophila melanogaster*, as well as for humans. One of the main questions in the field of neuroscience is, how does this kind of associative learning happen?

Fruit fly larvae can learn to associate a certain smell with a sugar reward. When a group of larvae learn to associate a smell with sugar, most but not all of them will approach that smell in the future. This shows associative learning in action, but it raises a big question. Did the larvae that failed to approach the smell fail to learn, or did they just happen to make a mistake finding the smell? Given another chance, would exactly the same larvae approach the smell as the first time? In other words, did all the larvae learn a little, or did some larvae learn completely and others learn nothing?

To find out, Lesar et al. built a computer-controlled maze to test whether individual fruit fly larvae liked or avoided a smell. Whenever a larva reached the middle of the Y-shaped maze, it could choose to go down one of two remaining corridors. One corridor contained air and the other carbon dioxide, a gas they would naturally avoid. Lesar et al. taught each larva to like carbon dioxide by activating reward neurons in its brain while filling the maze with carbon dioxide gas. Studying each larva as it navigated the maze revealed that they learn in a single jump, a 'lightbulb moment'. When Lesar et al. activated the reward neurons, the larva either 'got it' and stopped avoiding carbon dioxide altogether, or it did not. In the second case, it behaved as if it had received no training at all.

Classic and modern experiments on people suggest that humans might also learn in jumps, but research on our own brains is challenging. Fruit flies are an excellent model organism to study memory formation because they are easy to breed, and it is easy to manipulate their genetic code. Work in flies has already revealed many of the genes and cells responsible for learning and memory. But, to find the specific brain changes that explain learning, researchers need to know whether the animals they are examining have actually learned something. This new maze could help researchers to identify those individuals, making it easier to find out exactly how associative learning works.

preferences of differently trained groups of larvae. These assays quantify the effects of learning on a population level, but it is impossible to identify whether or to what extent an individual larva has learned.

New methods allow direct measurement of neural activity in behaving larvae (*Karagyozov et al., 2018; He et al., 2019; Vaadia et al., 2019*) and reconstruction of the connections between the neurons in a larva's brain (*Eichler et al., 2017; Eschbach et al., 2020a; Eschbach et al., 2020b; Takemura et al., 2017; Berck et al., 2016*), potentially allowing us to explore how learning changes the structure and function of this model nervous system. Using these tools requires us to identify larvae that have *definitively learned*. Recently, a device has been developed for assaying individual adult flies' innate (*Honegger et al., 2020*) and learned (*Smith et al., 2021*) olfactory preferences, but no comparable assay exists for the larval stage.

Further, to explore structural changes associated with learning, we need to form protein-synthesis dependent long-term memories (*Yin et al., 1995; Yin et al., 1994; Perazzona et al., 2004*). Larvae trained to associate odor with electric shock form memories that persist for at least 8 hr (*Khurana et al., 2009*). Odor-salt memories have been shown to partially persist for at least 5 hr (*Widmann et al., 2016; Eschment et al., 2020*) and can be protein-synthesis dependent (*Eschment et al., 2020*), depending on the initial feeding state of the larva. Overnight memory retention, whether or not requiring protein-synthesis, has not been demonstrated in the larva, nor has long-lasting retention of appetitive memories.

In this work, we demonstrate a new apparatus for in situ training and measurement of olfactory preferences for individual larvae. We use this assay to quantify appetitive memories formed by presentation of carbon dioxide (CO₂) combined with optogenetic activation of reward neurons. Using this device, we find that larvae are sensitive to both the timing and context of the reward presentation, that learning is quantized and all-or-none, and that repeated presentation of CO₂ without

reinforcer can erase a newly formed memory. We induce memories that persist overnight, and control whether these memories require protein synthesis through alteration of the training protocol.

Results

A Y-maze assay to characterize olfactory preferences of individual *Drosophila* larvae

Establishing the degree to which an individual larva seeks out or avoids an odorant requires repeated measurements of that larva's response to the odor. We developed a Y-maze assay (Buchanan et al., 2015; Werkhoven et al., 2019) to repeatedly test an individual's olfactory preference. The Y-mazes (Figure 1A) are constructed from agarose with channels slightly larger than the larvae, allowing free crawling only in a straight line (Heckscher et al., 2012; Sun and Heckscher, 2016). An individual larva travels down one channel and approaches the intersection with the other two branches of the maze. Here, the larva is presented with odorized air (or in this work, air containing CO₂) in one branch and pure air in the other. The larva then chooses and enters one of the two branches. This choice may be immediate or the result of a longer process in which the larva samples both channels and even reverses (Figure 1—video 2, Figure 1—video 3). When the larva reaches the end of its chosen channel, a circular chamber redirects it to return along the same channel to the intersection to make another choice. Custom computer vision software detects the motion of the larva while computer controlled valves manipulate the direction of airflow so that the larva is always presented with a fresh set of choices each time it approaches the intersection (Figure 1A, Figure 1—video 1).

We first sought to determine the suitability of this assay for measuring innate behavior. *Drosophila* larvae avoid carbon dioxide (CO₂) at all concentrations (Faucher et al., 2006; Jones et al., 2007; Kwon et al., 2007; Gershow et al., 2012). We presented larvae with a choice between humidified air and humidified air containing CO₂ each time they approached the central junction. At the 18% concentration used throughout this work, larvae with functional CO₂ receptors chose the CO₂-containing channel about 25% of the time. The probability of choosing the CO₂ containing channel increased as CO₂ concentration in that channel decreased (Figure 1F). *Gr63a*¹ (Jones et al., 2007) larvae lacking a functional CO₂ receptor were indifferent to the presence of CO₂ in the channel (Figure 1B), as were animals in which the CO₂ receptor neurons were silenced (*Gr21a>Kir.21*), indicating that larvae responded to the presence of CO₂ and not some other property of the CO₂ containing air stream. Silencing the Mushroom Body (*OK107>Kir.2.1*) did not impair innate CO₂ avoidance.

Pairing CO₂ presentation with optogenetic activation of a single pair of reward neurons eliminates CO₂ avoidance

Activation of the DAN-i1 pair of mushroom body input neurons has been shown to act as a reward for associative learning (Saumweber et al., 2018; Thum and Gerber, 2019; Schleyer et al., 2020; Weiglein et al., 2019; Eschbach et al., 2020b). In these experiments, the conditioned odor was innately attractive, but CO₂ is innately aversive. We wondered whether pairing DAN-i1 activation with CO₂ would lessen or even reverse the larva's innate avoidance of CO₂.

To train larvae in the same Y-maze used to measure preference, we manipulated the valves so that the entire chamber was either filled with humidified air or with humidified air mixed with additional CO₂, independent of the position of the larva, which was not tracked during training. At the same time, we activated DAN-i1 neurons expressing CsChrimson using red LEDs built in to the apparatus. For some larvae, we activated DAN-i1 when CO₂ was present (paired, Figure 1D). For others, we activated the reward neurons when only air was present (reverse-paired, Figure 1D). Each training cycle consisted of one 15 s CO₂ presentation and one 15 s air presentation, with DAN-i1 activated for the entirety of the CO₂ (paired) or air (reverse-paired) presentation phase. The training protocols schematized in Figure 1D were repeated for 20 successive cycles. Thus, for instance, in the reverse-paired scheme CO₂ offset at t=15s coincided with reward onset, and the reward offset at t=30s coincided with CO₂ onset at t=0 of the subsequent cycle.

For each larva, we first measured naive preference and then preference following training. We found that in the paired group, larvae became indifferent to CO₂ presentation following 20 training

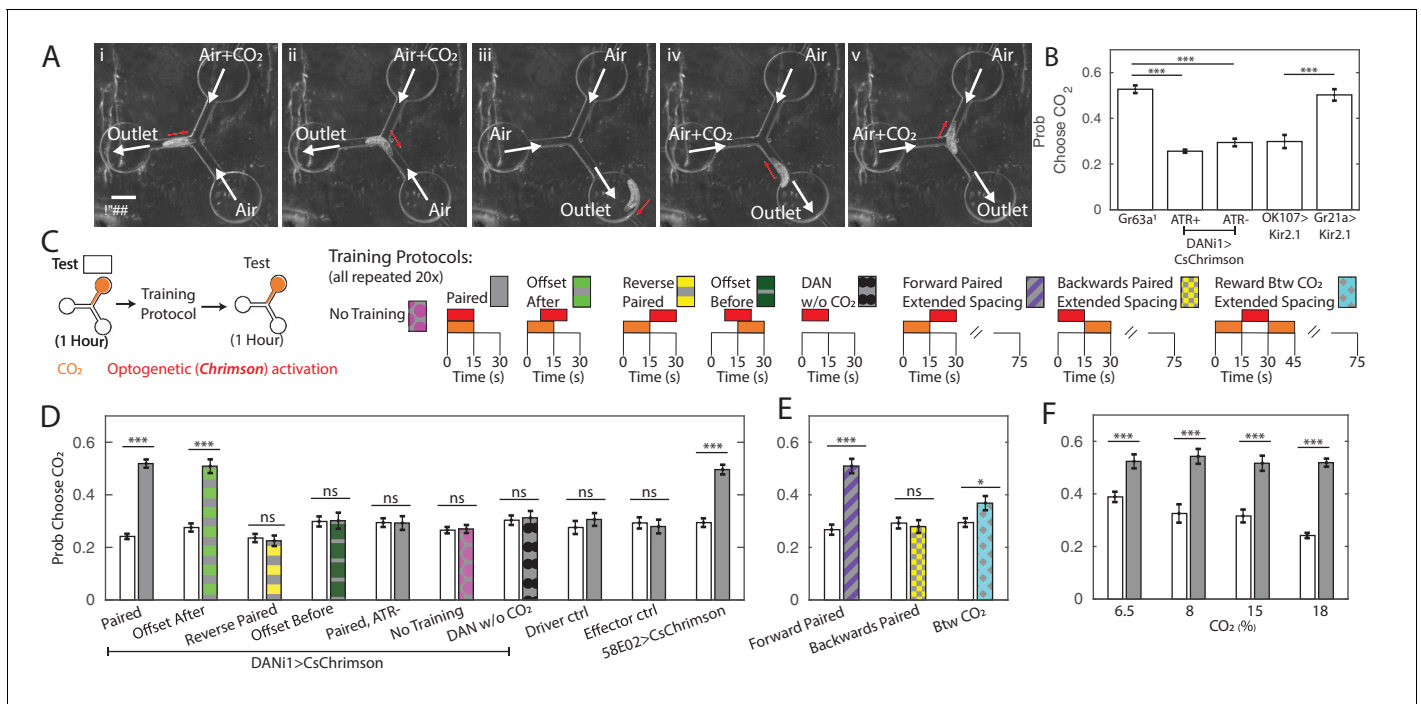


Figure 1. Y-maze assay to quantify innate and learned preference. (A) Image sequence of a larva making two consecutive decisions in the Y-maze assay. White arrows indicate direction of air flow; red arrow shows direction of larva's head. (B) Probability of choosing channel containing CO₂ without any training. (C) Schematic representation of experiments in (D, E, F). All larvae were tested in the Y-maze for 1 hr to determine initial preference and again following manipulation to determine a final preference. The manipulations were: Paired Training - reward in concert with CO₂ presentation, 15 s intervals, 20 repetitions; Offset After - reward presentation 7.5 s after CO₂ onset, 15 s intervals, 20 repetitions; Reverse-Paired Training - reward opposite CO₂ presentation, 15 s intervals, 20 repetitions; Offset Before - reward presentation 7.5 s before CO₂ onset, 15 s intervals, 20 repetitions; DAN Activation Without CO₂ - CO₂ is never presented, while reward is presented at 15 s intervals, 20 repetitions; no training - no manipulation between two testing periods; Forward Paired (extended spacing) - 15 s reward follows 15 s CO₂ presentation, followed by 60 s of air, 20 repetitions; Backwards Paired (extended spacing) - 15 s reward prior to 15 s CO₂ presentation, followed by 60 s of air, 20 repetitions; Reward Between CO₂ (extended spacing) - 15 s reward presentation between two 15 s CO₂ presentations, followed by 45 s of air, 20 repetitions. (D) Probability of choosing CO₂ containing channel before and after manipulation. All animals were fed ATR supplemented food, except those marked ATR-. (E) Probability of choosing CO₂ containing channel before and after training as a function of reward timing, in training protocols with extended air spacings. All animals were DANi1>CsChrimson and fed ATR. (F) Probability of choosing CO₂ containing channel before and after 20 cycles of paired training, as a function of CO₂ concentration, used both during training and testing. All animals were DANi1>CsChrimson and fed ATR. * p<0.05, ** p<0.01, *** p<0.001. The online version of this article includes the following video and source data for figure 1:

Source data 1. Spreadsheet containing each individual animal's decisions in temporal sequence.

Figure 1—video 1. Recording of a larva making 2 decisions within the Y-maze.

<https://elifesciences.org/articles/70317#fig1video1>

Figure 1—video 2. Recording of a larva before training, showing a sequence of decisions made at the Y-maze juncture.

<https://elifesciences.org/articles/70317#fig1video2>

Figure 1—video 3. Recording of a larva after training, showing a sequence of decisions made at the Y-maze juncture.

<https://elifesciences.org/articles/70317#fig1video3>

cycles (**Figure 1D**, DANi1>CsChrimson, Paired). We did not observe any change in preference in the reverse-paired group (DANi1>CsChrimson, Reverse-Paired). Nor did we observe a preference change following paired training for genetically identical animals not fed all-trans-retinal (ATR), a necessary co-factor for CsChrimson function (DANi1>CsChrimson, Paired ATR-). Animals fed ATR but not exposed to red light failed to show a preference shift (DANi1>CsChrimson, No Training). Larvae of the parent strains fed ATR and given paired training showed no preference shift (Effector Control, Driver Control). To control for possible effects of DAN-i1 activation, we activated DAN-i1 in 15 s intervals without presenting CO₂ at all during the training (DANi1>CsChrimson, DAN w/o CO₂); these larvae showed no shift in preference.

Taken together these results show that the change in CO₂ preference requires activation of the DAN-i1 neurons and is not due to habituation (Twick *et al.*, 2014; Das *et al.*, 2011; Larkin *et al.*, 2010), red light presentation, or other aspects of the training protocol. In particular, the paired and reverse-paired group experienced identical CO₂ presentations and DAN-i1 activations with the only difference the relative timing between CO₂ presentation and DAN-i1 activation.

Activation of DAN-i1 coincident with CO₂ presentation decreased larvae's subsequent avoidance of CO₂. Formally, this admits two possibilities: the larva's preference for CO₂ increased because CO₂ was presented at the same time as the reward or because CO₂ predicted the reward. To test whether learning was contingent on coincidence or prediction, we carried out an additional set of experiments. As before, we first tested innate preference, then presented 20 alternating cycles of 15 s of CO₂ followed by 15 s of air. However, this time during the conditioning phase, we either activated DAN-i1 7.5 s after CO₂ onset, in which case CO₂ predicted DAN-i1 activation, or 7.5 s before CO₂ onset, in which case CO₂ predicted withdrawal of DAN-i1 activation.

In both cases, DAN-i1 was activated in the presence of CO₂ for 7.5 s and in the presence of air alone for 7.5 s. If learning depended only on the coincidence between reward and CO₂ presentations, both should be equally effective at generating a change in preference. In fact, we only found an increase in CO₂ preference following training in which the CO₂ predicted the reward (Figure 1D).

Next, we asked whether reward prediction alone was sufficient to establish a memory, or if coincidence between CO₂ and DAN-i1 activation was also required. We altered the training protocol to present 15 s of CO₂ followed by 60 s of air. Some larvae were rewarded by activation of DAN-i1 in the 15 s immediately following CO₂ presentation (Forward Paired), while others were rewarded in the 15 s immediately prior to CO₂ presentation (Backwards Paired). For a third group of larvae, CO₂ was presented both before and after reward presentation (reward between CO₂ presentations). At no time was DAN-i1 activated in the presence of CO₂, but in the first group CO₂ predicted DAN-i1 activation while in the others it did not. We found an increased CO₂ preference for animals in this first group only (Figure 1E), indicating that reward prediction is both necessary and sufficient for learning in this assay.

In other associative conditioning experiments using DAN-i1 activation as a reward, decreased attraction to the odor was observed in the reverse-paired groups (Saumweber *et al.*, 2018; Thum and Gerber, 2019; Schleyer *et al.*, 2020). In our experiments, we did not see any evidence of increased aversion in the reverse-paired groups.

Untrained larvae avoided CO₂. After 20 cycles of paired, offset-after, or forward-paired training, larvae no longer avoided CO₂, but they also did not seek it out. We wondered whether it might be possible to train larvae to develop an attraction to the innately aversive CO₂. In other contexts, reward via activation of 3 DANs (DAN-i1, DAN-h1, DAN-j1 - whether DAN-h1 is present in second instar larvae, used in this study, is presently unreported) labeled by the 58E02-Gal4 line has been reported to produce strong learning scores (Saumweber *et al.*, 2018; Rohwedder *et al.*, 2016; Lyutova *et al.*, 2019; Schleyer *et al.*, 2020). We repeated the training protocol, substituting 58E02 activation for DAN-i1 activation alone, but did not see an increased preference following training compared to DAN-i1 activation alone (Figure 1D, 58E02>CsChrimson).

Next, we asked how varying the CO₂ concentration might affect animals' performance in the assay. We presented lower concentrations of CO₂ both during the training and testing phases, and found that decreasing the CO₂ concentration decreased innate avoidance of CO₂. In all cases, following training, larvae lost avoidance to CO₂ but none showed statistically significant attraction (Figure 1F).

Learning is quantized and all-or-none

We investigated how change in preference for CO₂ following associative conditioning with DAN-i1 activation depended on the amount of training. As in the previous experiments, we first measured the innate preference, then trained each larva using repeated cycles alternating pure and CO₂ containing air, while activating DAN-i1 in concert with CO₂ presentation. In these experiments, however, we varied the number of training cycles an individual larva experienced. We found that as a group, larvae that had experienced more training chose the CO₂ containing channel more often (Figure 2A).

Our data showed that increasing the amount of training increased overall preference for CO₂ up to a saturation point. But what was the mechanism for this change? Did each cycle of training

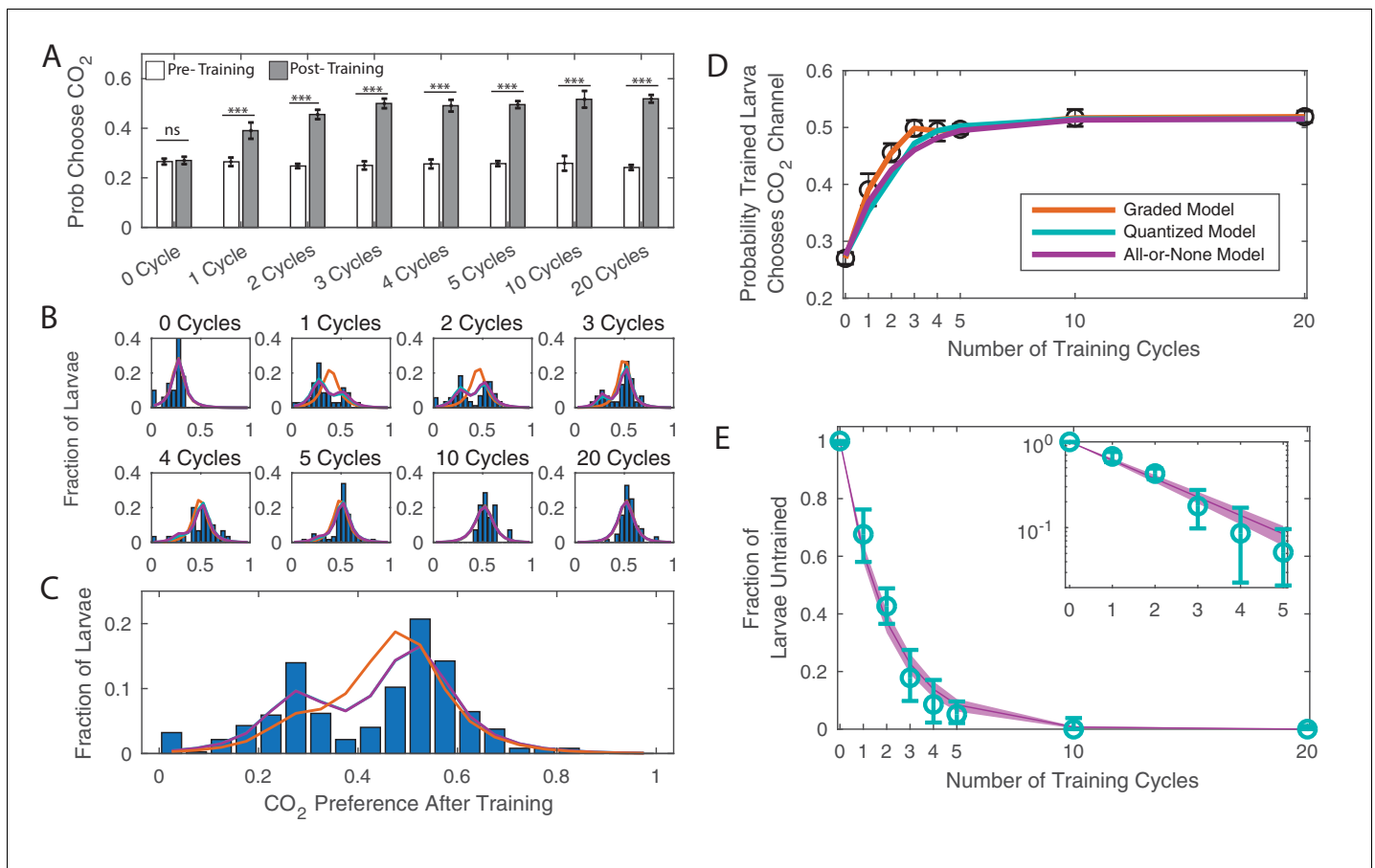


Figure 2. Dose dependence of learning DANi1>CsChrimson were given varying cycles of paired training (as in **Figure 1C**). (A) Probability of choosing CO₂ containing channel before and after training, as a function of amount of training. *** $p < 0.001$. (B) Histograms of individual larva preferences after training, grouped by number of training cycles. (C) Histogram of individual larva preference after training for all larvae. (D) Population average probability of choosing CO₂ following training vs. dose. (E) Fraction of larvae untrained vs. number of training cycles. Teal: fit parameters and error ranges from quantized model, purple lines, prediction and error ranges from memoryless model. Note logarithmic y-axis on insert. (C–E) Orange: graded model prediction - post-training preference is represented by a single Gaussian distribution whose mean and variance depend on amount of training; Teal: quantized model prediction - post-training preference is represented by two fixed Gaussian distributions and the fraction of larvae in each population depends on the amount of training; Purple: all-or-none model prediction - post-training preference is represented by two fixed Gaussian distributions and the effect of a single training cycle is to train a fixed fraction of the remaining untrained larvae. The online version of this article includes the following source data for figure 2:

Source data 1. Spreadsheet containing each individual animal's decisions in temporal sequence.

increase each larva's preference for CO₂ by some small amount, with the effect accumulating over repeated training (graded learning)? Or did some larvae experience a dramatic preference change – from naive to fully trained – with each cycle of training, with the number of fully trained larvae increasing with training repetitions (quantized learning)?

Either quantized or graded learning can explain the shift of mean preference of a population (**Gallistel et al., 2004**); to differentiate between the modes of learning, we examined repeated decisions made by individual animals, measurements that were impossible in previous larval assays. For each larva, we quantified the change in CO₂ preference before and after training. **Figure 2B** shows a histogram of larva preference (the fraction of times an individual larva chose the CO₂ containing channel) after training, grouped by the number of cycles of training a larva received.

Larvae that received no training (0 cycles) formed a single population that chose CO₂ 27% of the time. Larvae that were trained to saturation (20 training cycles) also formed a single group centered around 52% probability of choosing CO₂. Both the graded and quantized learning models make the same predictions for these endpoints, but their predictions vary starkly for the intermediate cases. A

graded learning model predicts that all larvae that received the same amount of training would form a single group whose mean preference for CO₂ would increase with increasing training. A quantized learning model predicts that larvae that have received the same amount of training will form two discrete groups ('trained' and 'untrained') with fixed centers whose means do not depend on the amount of training. With increased training an increasing fraction of larvae would be found in the trained group.

We fit the distributions of preference following conditioning to graded and quantized learning models. In the graded model, the preference was represented by a single Gaussian distribution whose mean and variance were a function of amount of training (orange, **Figure 2**). In the quantized model, the preference was represented by two Gaussian distributions; the fraction of larvae in each population was a function of the amount of training (teal, **Figure 2**).

We found that the data were better described by the quantized learning model (Table 4): larvae form two discrete groups, with the fraction in the trained group increasing with each cycle of additional training. The centers of the two groups do not vary with the amount of training, a point made most clear by considering the preference after training of all larvae taken together regardless of the amount of training received (**Figure 2C**), which shows two well defined and separated groups. From these data, we concluded that the effect of our associative conditioning on an individual larva is to either cause a discrete switch in preference or to leave the initial preference intact.

Next we asked what effect, if any, associative conditioning had on larvae that retained their innate preferences following training. Whether humans form associative memories gradually through repeated training or learn in an all-or-none manner has been the subject of debate in the Psychology literature (**Roediger and Arnold, 2012**); recent electrophysiological measurements in humans supports the all-or-none hypothesis (**Ison et al., 2015**). If learning is all-or-nothing, then if a larva has received training but has not yet expressed a behavioral switch, it is the same as if the larva has received no training at all. In this case, with every training cycle, regardless of past experience, every untrained larva will have the same probability of learning: ρ , and the effect of training can be described by a particularly simple equation

$$n_u(i+1) = n_u(i) - \rho n_u(i) \quad (1)$$

where $n_u(i)$ are the number untrained larvae following i cycles of training. Note that ρ can depend on the training protocol or other external variables, but it does not depend on the past training experiences of the larvae, and can be considered a fixed constant for a given experimental condition. The solution to this equation is an exponentially decaying population of untrained larvae. For a given initial population $n_u(0)$ of untrained larvae,

$$n_u(i) = (1 - \rho)^i n_u(0) \quad (2)$$

Any so-called memoryless process like this produces an exponential decay of the initial population (**Apostol, 1969**). Meanwhile, processes with memory can produce other distributions. For example, if the training were *cumulative*, we would expect a threshold effect: as the number of cycles of training increased from 0, most larvae would initially remain untrained until a critical number of cycles (n_c) were reached and there would be a sudden shift to a mostly trained population. While a process with memory can also produce exponential decay (e.g. if each larva required a fixed n_c cycles of training to learn, and n_c was itself exponentially distributed), all memoryless processes must produce an exponential decay, and exponential decay is therefore an indicator of a memoryless (all-or-none) process.

Our fit to the quantized learning model produces an estimate of the fraction of larvae that remain untrained following training. We plotted the fraction of untrained larvae vs. number of training cycles and saw that the fraction of larvae in the untrained group exponentially decreased with increasing training (**Figure 2E**, note logarithmic y-axis on insert). We then fit the population distributions to an all-or-none quantized learning model in which the effect of a single training cycle was to train a fixed fraction of the remaining untrained larvae (purple, **Figure 2**). This model fit the data better than the graded learning model and almost as well as the original quantized learning model (in which the fraction of untrained larvae was fit separately to each group) despite having fewer parameters than either model. According to standard selection rules (BIC and AIC), the all-or-none quantized model best describes the data (Table 4).

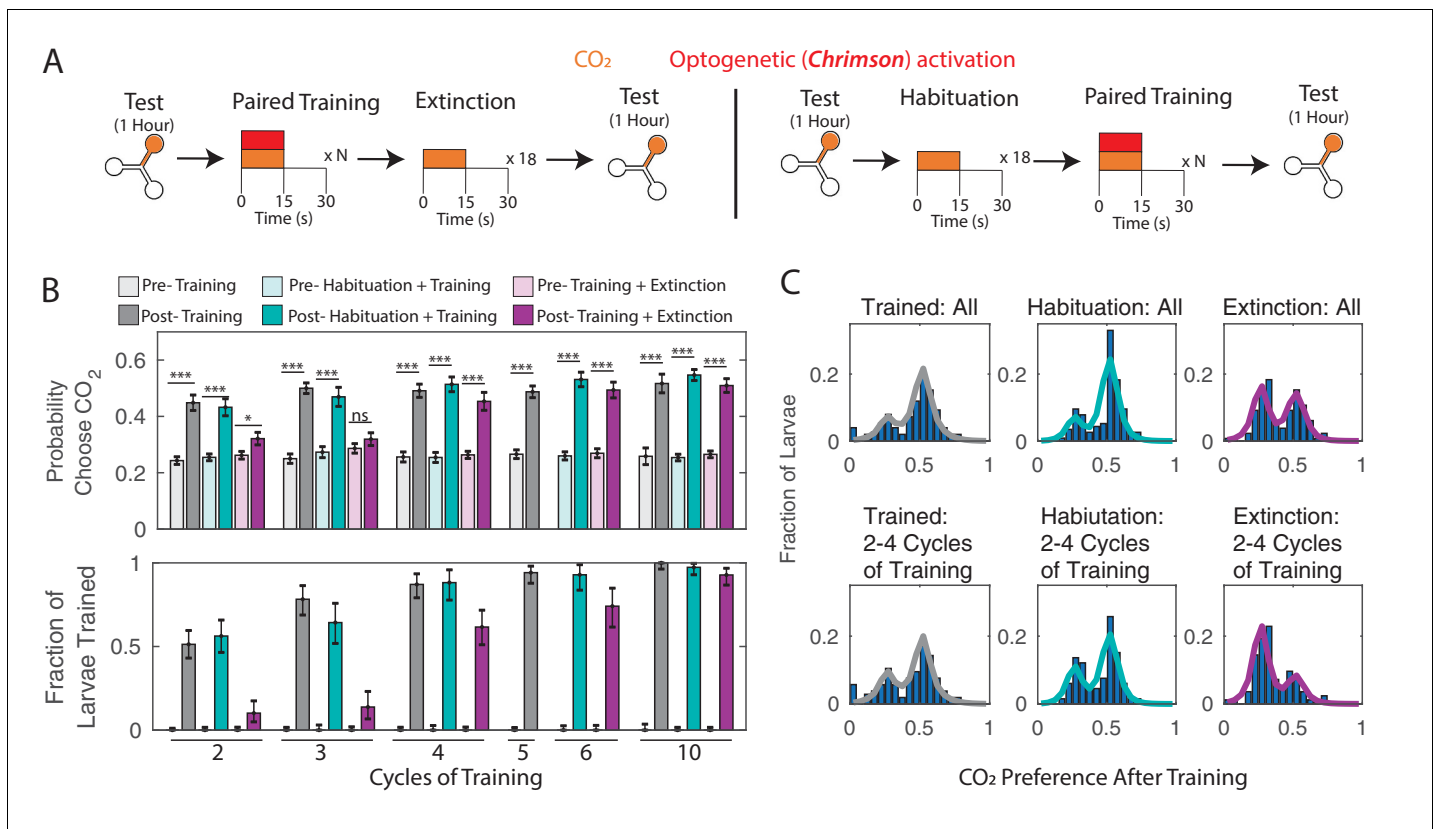


Figure 3. Memory extinction (A) Testing and training protocols for B,C. Training + Extinction: larvae were exposed to 18 cycles of alternating CO₂ and air following training. Habituation + Training: larvae were exposed to 18 cycles of alternating CO₂ and air prior to training. (B) Probability of choosing CO₂ containing channel (top) and fraction of larvae in trained group according to double Gaussian model fit (bottom) before and after training scheme. (C) Histograms of individual larva preference after training, for all larva and for larva trained with 2–4 training cycles. * p < 0.05, ** p < 0.01, *** p < 0.001. The online version of this article includes the following source data and figure supplement(s) for figure 3:

Source data 1. Spreadsheet containing each individual animal's decisions in temporal sequence.

Figure supplement 1. After extinction, larvae can be trained again.

Figure supplement 2. Larvae population average response following training.

Figure supplement 3. Larvae given additional training between testing periods.

Repeated exposure without reward following training leads to memory extinction

Reversal learning, in which the reward contingency is reversed, and extinction, in which the conditioned stimulus is presented without reward, experiments explore cognitive flexibility. Previous experiments with both adult *Drosophila* (Tully et al., 1990; Ren et al., 2012; Wu et al., 2017; Vogt et al., 2015) and larval (Mancini et al., 2019) *Drosophila* demonstrated a reversal learning paradigm. Extinction has been demonstrated in adult flies (Felsenberg et al., 2017; Felsenberg et al., 2018; Schwaerzel et al., 2002) but not in larvae.

To test for extinction, we again first measured an individual larva's CO₂ preference and then carried out associative conditioning for a given number (2–10) of training cycles. Next instead of immediately testing the larva's new preference for CO₂, we exposed the larva to an extinction phase – 18 cycles of alternating CO₂ and air without any optogenetic reward. Following the extinction period, we tested larvae as usual to measure their changed preference for CO₂. As a control against the effects of increased CO₂ exposure, we also performed habituation experiments, which were the same as the extinction experiments, except the 18 unrewarded cycles were presented prior to the rewarded training cycles. The extinction and habituation protocols are schematized in Figure 3A.

When we compared the 'habituated' groups of larvae to larvae trained for the same number of cycles without habituation or extinction, we found that unrewarded CO₂ presentation prior to

training had no effect on the eventual preference change (**Figure 3B**). This was unsurprising, as the initial testing period already offered a number of unrewarded CO₂ presentations. In contrast, unrewarded CO₂ presentations following training reversed the effect of training; for small (2 or 3 cycles) amounts of training, the reversal was almost complete (**Figure 3B**).

We previously observed that associative conditioning produced a discrete and quantized change in CO₂ preference. Here, we found that extinction following training greatly reversed the effects of conditioning. We wondered whether larvae that had been subject to both training and extinction reverted to their original CO₂ preference or to an intermediate state. In the former case, we would expect to see a bimodal distribution of preference change following training and extinction, while in the latter we would see a third group of larvae. This group would be most evident in experiments where two to four cycles of training were followed by extinction, as these had the largest deficit in the fraction of trained larvae compared to habituated larvae that received the same amount of training. We examined the preferences of all larvae following two to four cycles of training, grouped by whether they were normally trained, habituated, or subject to extinction (**Figure 3C**). In all cases, we observed two groups with the same central means and no evidence of a third intermediate group. We concluded that larvae subject to training then extinction reverted to their 'untrained' state.

We wondered whether larvae would still learn if they received additional training directly following extinction. As before, we measured the innate preference, presented three paired training cycles followed by the extinction phase. At this point, based on our previous results, larvae would have returned to their initial innate avoidance of CO₂. We then immediately presented three more paired training cycles before behavioral testing (**Figure 3—figure supplement 1A**). We found that following this training-extinction-training protocol, both the population preference for CO₂ (**Figure 3—figure supplement 1B**) and the fraction of larvae trained (**Figure 3—figure supplement 1C**) were comparable to larvae that had been trained three times without extinction cycles.

Given the relatively short duration of training and the ability of unrewarded CO₂ presentations to extinguish prior training, we wondered whether larvae might change their CO₂ preferences over the course of the hour-long post-training behavioral readout. In particular, might the apparent threshold of 50% attraction be an artifact due to a short period of attraction to CO₂ followed by a longer period of indifference or modest avoidance?

To test for a short period of increased attraction immediately following training, we reanalyzed the results of experiments with 2, 5, and 20 cycles of paired training. In each case, we compared the initial 10 min of the post-training choice assay to the final 50 min (**Figure 3—figure supplement 2A**) and found no significant difference between the initial and final periods for any of these training conditions. We then compared the mean preference over the first five choices (representing five unrewarded CO₂ presentations) made by each larva to the mean preference in the remainder of the experiment and again found no significant difference (**Figure 3—figure supplement 2B**). Breaking the behavioral readout into equal 15 min periods also reveals no strong temporal signal (**Figure 3—figure supplement 2C–E**).

Finally, we developed a new protocol to minimize the possible effects of extinction over the course of the behavioral readout, using the fact that training following extinction can re-establish a lost memory (**Figure 3—figure supplement 1**). We trained each larva with 10 paired cycles (5 min of training), then tested their preference for 15 min, then presented another 10 paired training cycles followed by another 15 min of testing, for a total of 4 training and testing blocks (**Figure 3—figure supplement 3**). The results were comparable to when we presented a single training block followed by an hour-long test period. Thus, we concluded that the apparent limit of 50% population preference to CO₂ following training was not due to the long time-scale of the behavioral readout.

Larvae can retain memory overnight; the type of memory formed depends on the training protocol

Studies in adult (Tully et al., 1990; Yin et al., 1995; Margulies et al., 2005) and larval (Honjo and Furukubo-Tokunaga, 2005; Honjo and Furukubo-Tokunaga, 2009; Widmann et al., 2016; Khurana et al., 2009; Eschment et al., 2020; Aceves-Piña and Quinn, 1979) *Drosophila* have identified distinct memory phases: short-term memory (STM), middle-term memory (MTM), long-term memory (LTM), and anesthesia-resistant memory (ARM). LTM and ARM are consolidated forms of memory controlled by partially separate molecular and anatomical pathways (Isabel et al., 2004; Jacob and Waddell, 2020; Wu et al., 2012). ARM is resistant to anesthetic agents (Quinn et al.,

1974); LTM requires cAMP response element-binding protein (CREB)-dependent transcription and de-novo protein synthesis, while ARM does not (Yin *et al.*, 1995; Perazzona *et al.*, 2004). Adults have been shown to retain memories for up to a week (Yin *et al.*, 1995). Larvae trained to associate odor with electric shock form memories that persist for at least 8 hr (Khurana *et al.*, 2009). Odor-salt memories have been shown to persist for at least 5 hr (Widmann *et al.*, 2016; Eschment *et al.*, 2020) and can be either ARM or LTM, depending on the initial feeding state of the larva.

We sought to determine whether we could create consolidated memories that would persist overnight, and if so, whether these memories represented ARM or LTM. As in previously described experiments, we first tested each larva's individual preference in the Y-maze assay, trained it to associate CO₂ presentation with DAN-i1 activation, and then measured its individual preference again following training. After this second round of testing, we removed the larva from the apparatus and placed it on food (without ATR) overnight. The next day, we placed the larva back in the Y-maze and again tested its preference for CO₂, without any additional training.

We found that following 20 cycles of training, larvae became indifferent to CO₂ and this indifference persisted to the next day. Similarly, we found that most larvae switched preference following five cycles of training and retained that preference overnight. Larvae that received no training or 20 cycles of unpaired training had no change in CO₂ preference immediately following training or the next day (Figure 4B).

We had previously shown two cycles of training caused roughly half the larva to change preference immediately after training. We decided to use this partition to verify a correlation between immediate and long-term memories; we expected that larvae initially in the 'trained' group would also form a 'trained' group the following day. However, while we found that two cycles of training were sufficient to cause some larvae to become indifferent to CO₂ immediately following training, when we tested these larvae the next day, we found that all had reverted to their initial avoidance of CO₂.

There were two possible explanations for this reversion. Perhaps, two cycles of training were sufficient to form a short term memory, but more training was required to induce a long-term memory. Or perhaps the testing period, in which larvae were exposed repeatedly to CO₂ without reward, reversed the two-cycle training. To control for the latter, we modified the experimental protocol. We tested each larva's innate preference, presented two training cycles, and then immediately removed the larva to food overnight, without any further testing. When we tested these larvae the next day, we found that they showed decreased avoidance of CO₂. This indicated that two cycles of training were sufficient to form a memory lasting overnight, but that immediate exposure to unrewarded CO₂ following this short training interval likely reversed the effects of training, an effect we observed in Figure 3. When larvae were trained for 20 cycles, omitting the testing had no effect on these larvae's preferences the following day.

To confirm that extinction could explain the failure to form a persistent memory, we exposed larvae to three cycles of paired training, then 18 cycles of extinction (as in Figure 3) and then removed them to food overnight before testing their preferences the next day. As expected, these larvae avoided CO₂ as much the next day as they did prior to training (Figure 4B, Ext Post-Train).

We wondered whether memories that had consolidated overnight would be more resistant to extinction. We repeated the previous experiment with a single modification. As before, we tested the larva's initial preference and trained it with three cycles of rewarded CO₂ presentation. This time, we immediately removed the larva to food following training. The next day, we returned the larva to the Y-maze and presented the extinction phase of 18 unrewarded CO₂ presentations prior to testing for CO₂ preference. We found that in this case, larvae still expressed an increased preference for CO₂ despite the extinction phase (Figure 4B, Ext Pre-Test). The only difference between the two experiments was whether we attempted extinction immediately after training or the next day. Thus, we concluded that overnight consolidation made memories more resistant to extinction.

ARM can be distinguished from LTM because the latter requires de novo protein synthesis and can be disrupted by ingestion of the translation-inhibitor cycloheximide (CXM). To incorporate CXM feeding, we modified our protocols. Instead of raising larvae on ATR supplemented food, we raised them on standard food and then fed them with ATR supplemented yeast paste for 4 hr prior to the experiment (ATR+/CXM-). For some larvae (ATR+/CXM+), we also added CXM to the yeast paste. In this way, we could be sure that if ATR+/CXM+ larvae ingested enough ATR to allow for CsChrimson activation of DAN-i1, they must have also ingested CXM as well. To further verify CXM

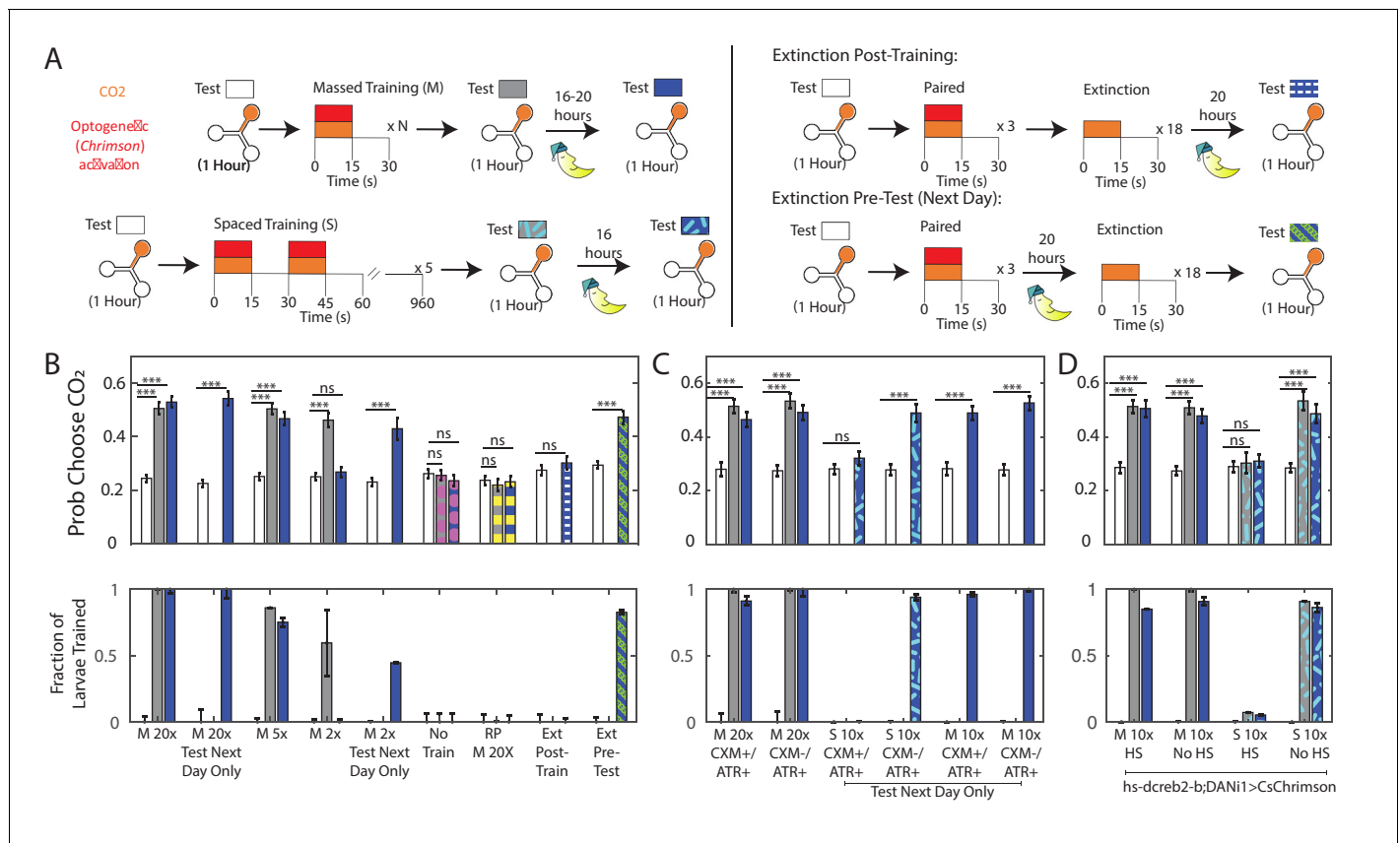


Figure 4. Memory retention overnight. (A) Testing and training protocols. Except where indicated, larvae were tested, trained immediately after testing, tested again, then placed on food overnight and tested the following day. For extinction experiments, larvae were trained three times, and then exposed to 18 cycles of alternating CO₂ and air either immediately following training or prior to testing the next day. (B,C,D) Probability of choosing CO₂ containing channel (top) and fraction of larvae in trained group according to double Gaussian model fit (bottom) prior to training, immediately following training, and the next day. When the center bar is missing, larvae were not tested immediately following training but instead removed immediately to food. M Nx = massed training, N repetitions, S 10x = spaced training 10 total pairings, RP = reverse paired (see **Figure 1C**), No Train = no training. Larvae in (B,C) were DAN1>CsChrimson. Larvae in (D) were DAN1>hs-dCREB2-b;CsChrimson. Larvae were raised on food containing ATR, except for ATR+/CXM-, ATR+/CXM+ larvae who were fed ATR supplemented yeast paste (without/with cycloheximide) for 4 hr prior to initial testing. For reverse-paired (RP) and no training schemes, see **Figure 1B**. * p<0.05, ** p<0.01, *** p<0.001.

The online version of this article includes the following source data for figure 4:

Source data 1. Spreadsheet containing each individual animal's decisions in temporal sequence.

ingestion, we placed ATR+/CXM+ and ATR+/CXM- larvae on clean food and allowed them to continue development. 95% of ATR+/CXM- larvae pupated, while only 45% of ATR+/CXM+ larvae pupated.

Following the 4 hr feeding period, ATR+/CXM+ and ATR+/CXM- larvae were treated identically. As in the previously described experiments, we first tested each larva's individual preference in the Y-maze assay, trained the larva 20 times to associate CO₂ presentation with DAN-1 activation, and then measured its individual preference again following training. After this second round of testing, we removed the larva from the apparatus and placed it on food (without ATR or CXM) overnight. The next day we placed the larva back in the Y-maze and again tested its preference for CO₂, without any additional training.

We found that performances tested immediately and 16 hr after training were both unaffected by CXM treatment. Following 20 cycles of training, larvae from both groups (ATR+/CXM+; ATR+/CXM-) became indifferent to CO₂ and this indifference persisted to the next day (**Figure 4C**). This suggests that the memory formation was independent of de novo protein synthesis.

In adult *Drosophila*, whether ARM or LTM is formed depends on the training protocol (Tully et al., 1990; Tully et al., 1994; Yin et al., 1995; Yu et al., 2006; Bouzaiane et al., 2015).

'Massed' training, in which all conditioning occurs in rapid sequence without rest intervals, results in ARM, while 'spaced' training, in which the conditioning occurs in blocks separated by intervals of time, produces LTM. Our training protocol more closely resembles massed training, so it seemed sensible that it would produce ARM. To see if we could instead develop LTM, we established a spaced training protocol. Larvae received two paired cycles of training, followed by a 15-min interval of air-presentation only; this sequence was repeated five times. To keep the total length of the experiment within a (covid-related) limited daily time window, we did not test the larvae immediately after training but only the next day.

Prior to spaced training, both ATR+/CXM- and ATR+/CXM+ larvae avoided CO₂ to the same degree. We found that 1 day following spaced training, ATR+/CXM+ larvae continued to avoid CO₂, while ATR+/CXM- larvae did not. This indicated that spaced training formed a memory whose retention was disrupted by CXM. To verify that spacing the trials was essential to forming a protein-synthesis dependent memory, we duplicated the experiments exactly, except we presented 10 cycles of training *en masse*, rather than spacing them. In this case, both ATR+/CXM- and ATR+/CXM+ larvae expressed learned indifference to CO₂ 1 day following training (**Figure 4C**).

As an alternate to CXM feeding, LTM (but not ARM) formation can also be disrupted through use of hs-dCREB2-b, a heat-shock inducible dominant-negative repressor of transcription mediated by dCREB2-a. (*Perazzona et al., 2004; Yin et al., 1995*). Specifically, in adult flies expressing hs-dCREB2-b, memory retention is disrupted in a heat-shock-dependent manner following spaced, but not massed training (*Yin et al., 1995*). We therefore repeated our long-term memory experiments in larvae that in addition to expressing Chrimson in DAN-i1 neurons also carried the hs-dCREB2-b transgene. Massed and spaced training were carried out as previously described, using larvae raised on ATR supplemented food, except that some larvae (HS) received a 30 min heat-shock (at 37 C), followed by a 30 min recovery period (at 25 C) immediately prior to the beginning of the experiment (i.e. prior to the initial testing of naive preference). Preference for CO₂ was tested prior to training, immediately following training, and the next day, following an overnight rest on food without ATR.

We found that, congruent with our CXM experiments, the day after spaced training, heat-shocked larvae (**Figure 4D,S 10x, HS**) avoided CO₂ to the same extent they did prior to training, while larvae that were not heat-shocked (**Figure 4D,S 10x, No HS**) retained learned indifference; larvae that received massed training (**Figure 4D,M 10x, HS and No HS**) retained their learned indifference overnight, regardless of heat-shock. These results are consistent with similar experiments in adult flies (*Yin et al., 1994; Yu et al., 2006*).

Immediately following spaced training (80 min after the initiation of the spaced training protocol), heat-shocked larvae continued to avoid CO₂, showing that memory formation was impaired on a relatively short timescale. This is consistent with previous work in the larva, where dCREB2-b expression induced memory deficits beginning 30 min following a single 30 min training cycle (*Honjo and Furu-kubo-Tokunaga, 2005*), and immediately following 125 min of spaced training (*Widmann et al., 2016*). In those experiments, neither training protocol was shown to induce a persistent long-term memory.

Discussion

In this work, we demonstrated a new apparatus for training individual larvae and assessing their olfactory preferences. Compared to the existing paradigm, our assay allows for measuring individual animals' changes in preference due to training, allows for greater control of the temporal relation between the conditioned and unconditioned stimuli, and does not require any handling of the animals between training and testing.

In our assay, larvae learned in a switch-like (all-or-none two-state quantized) manner. The learning process was better described as a sudden transition between states than as a graded change in preference, and each cycle of training (presentation of CO₂ coupled with reward) either caused a state transition or did not. Pigeons, rats, and rabbits have all been shown to experience sudden performance increases in learning tasks, suggesting quantized learning may be a generalized phenomenon (*Gallistel et al., 2004*). We found no evidence of a cumulative effect of prior training in the probability that a given cycle of training would induce a state transition in larvae that had not already transitioned. We did, however, find evidence that repeated cycles of training stabilized memories against

later extinction effected by presentation of CO₂ without reward. These measurements were enabled by our assay's ability to track individual preferences over the course of the entire experiment.

We directly tested the ability of unrewarded CO₂ presentations to extinguish a just-formed memory by presenting CO₂ without air immediately following training (**Figure 3**). We also indirectly measured the effects of extinction due to unrewarded CO₂ presentation during the hour-long behavioral test (**Figure 3—figure supplement 2**). Following two cycles of training, immediate presentation of 18 unrewarded CO₂ cycles abolished the formed memory (**Figure 3B**), but without this direct extinction protocol, we saw no evidence of extinction over the course of the hour-long behavioral test (**Figure 3—figure supplement 2A–C**). It is perhaps unsurprising that rapid and consistent unrewarded presentations immediately following training are more effective at extinguishing a memory than the later and more varied unrewarded presentations during the behavioral test. But following two cycles of training, the behavioral test does prevent expression of the formed memory the next day (**Figure 4B**). This could show that the unrewarded presentations during behavioral testing are too late and/or sporadic to prevent immediate memory expression but do prevent the transition to more long-lived ARM. Further study will be required to confirm this. Our apparatus can precisely control the timing and nature of both rewarded and unrewarded presentations to probe different phases of memory formation and consolidation.

We found that larvae trained in our assay retained memories overnight: 16–20 hr. When training was presented all at once, these memories were not disrupted by ingestion of the protein-synthesis inhibitor cycloheximide or induction of the transcription repressor dCREB2-b, while when training was spaced over time, cycloheximide feeding and dCREB2-b induction both prevented long duration memory formation. Thus, we identified spaced training as producing long-term memory (LTM) and the massed training as producing anesthesia-resistant memory (ARM). These results are the first demonstrations that larvae can retain memories overnight; they are entirely congruent with observations in adult flies.

We explored how the order of CO₂ and reward presentations affected learning. We found that for larvae to learn, CO₂ onset must occur coincident with or before reward onset, but that it was neither necessary nor sufficient for CO₂ and reward to be presented together at the same time. While we assume that the same neural mechanism underlies learning in the 'paired', 'offset after' (**Figure 1D**) and 'forward-paired' (**Figure 1E**) paradigms, it is at least formally possible that the mechanism might be different in these contexts. Most of the work in this paper used the 'paired' protocol; it would be interesting to test in the future whether the 'forward-paired' protocol produces memories that differ in their resistance to extinction or in their long-term persistence.

Our results using the 'reverse paired' (**Figure 1D**) and 'backwards paired' (**Figure 1E**) protocols differed from previous reports. In other assays, presenting the reward (including via activation of DAN-i1) prior to presenting the conditioned odor results in *decreased* attraction/*increased* avoidance (**Schleyer et al., 2020; Saumweber et al., 2018**) of that odor. We found that such 'reverse-pairings' neither increased nor decreased a larva's avoidance of CO₂. There are a number of differences, most significantly our new behavioral assay and our use of the innately aversive CO₂ as the conditioned stimulus that might account for the discrepancy.

While this work does not directly speak to the neural mechanism behind the change in preference, it is congruent with the evolving model of learning in *Drosophila*. In this model, different Mushroom Body Output Neurons (MBONs) promote approach or avoidance (**Aso et al., 2014; Eschbach and Zlatic, 2020; Perisse et al., 2013; Oswald et al., 2015; Oswald and Waddell, 2015; Hige et al., 2015**) and synapse onto a convergence neuron that integrates their activities (**Eschbach and Zlatic, 2020**). Prior to learning, aversive and appetitive MBONs are thought to receive similar drives from Kenyon Cells (KCs) that respond to specific olfactory signals. That is, in response to a stimulus, the activities of MBONs representing these opposite valences are initially balanced, and behavior is governed by an innate preference to that odor, controlled by neuronal circuits external to the MB (**Aso et al., 2014; Eschbach and Zlatic, 2020**). Aversive and appetitive learning depress the odor drive to appetitive and aversive MBONs, respectively: learning that a stimulus is appetitive weakens the connection between KCs encoding that stimulus and the avoidance MBONs, promoting approach, while aversive conditioning weakens the connection between KCs and approach MBONs, promoting avoidance (**Aso et al., 2014; Oswald and Waddell, 2015; Eschbach and Zlatic, 2020**).

According to this model, presentation of CO₂ coincident with or prior to the activation of DAN-i1 reduces the ability of CO₂ to excite one or more aversive MBONs, likely including MBON-i1, which encodes avoidance (*Eschbach and Zlatic, 2020*) and is postsynaptic to DAN-i1 (*Eichler et al., 2017*). This results in an appetitive drive from the MB that cancels out the innate avoidance pathway. Why in our experiments the learned appetitive drive appears to exactly cancel but not overcome the innate aversion should be the subject of further study; it may be a simple coincidence or artifact of the experimental protocol, or it may reflect more profound circuit principles.

Understanding memory formation at the circuit and synaptic levels simultaneously is a heroic task, even aided by the larva's numerically simple nervous system and the tools (including EM-reconstruction) available in the larva. The work here represents progress toward this goal. We demonstrate long-term protein synthesis dependent memory, implying that memories are encoded in synaptic change. Our assay allows us to precisely identify those individuals who have formed long-term memories. Animals are found in only two behavioral states: innate avoidance or learned indifference; this likely reflects two discrete states of the underlying neural circuit.

Our associative conditioning paradigm pairing CO₂ presentation with DAN-i1 activation has experimental advantages for circuit-cracking. The conditioned stimulus is sensed by a single pair of genetically identified sensory neurons; the unconditioned stimulus is provided by activation of a single pair of genetically identified reward neurons whose connectivity has been fully reconstructed (*Schleyer et al., 2020*). How the larva navigates in response to CO₂ presentation has been described in detail (*Faucher et al., 2006; Gershow et al., 2012; Gepner et al., 2015; Gepner et al., 2018*), as has how neurons downstream of DAN-i1 and the KCs contribute to navigational decision making (*Eichler et al., 2017; Saumweber et al., 2018; Thum and Gerber, 2019; Schleyer et al., 2020*). This is a particularly favorable starting point to understand how synaptic plasticity due to associative conditioning leads to changes in circuit function that effect changed behavioral outcomes.

Conclusion

We introduced a Y-maze assay capable of measuring the olfactory preferences of individual larval *Drosophila* and of in situ associative conditioning. We found that when larvae learn to associate CO₂ with reward neuron activation, the result is a switch from innate avoidance to learned indifference, with no intervening states. We demonstrated a protocol to form stable protein-synthesis dependent long term memories. This provides a strong starting point for 'cracking' a complete olfactory learning circuit.

Materials and methods

Key resources table

Reagent type (species) or resource	Designation	Source or reference	Identifiers	Additional information
Genetic reagent (<i>D. melanogaster</i>)	w[1118]; P{y[+t7.7]w[+mC]=20XUAS-IVS-CsChrimson.mVenus}attP2 (w;;UAS-CsChrimson)	Bloomington Stock Center	RRID:BDSC_55136	
Genetic reagent (<i>D. melanogaster</i>)	SS00864 split-Gal4 (DAN-i1-Gal4)	<i>Saumweber et al., 2018</i>		Gift of Marta Zlatic, Janelia Research Campus
Genetic reagent (<i>D. melanogaster</i>)	w[*]; Gr63a[1]	Bloomington Stock Center	RRID:BDSC_9941	
Genetic reagent (<i>D. melanogaster</i>)	w[1118]; P{y[+t7.7]w[+mC]=GMR58E02-GAL4}attP2 (GMR58E02-Gal4)	Bloomington Stock Center	RRID:BDSC_41347	
Genetic reagent (<i>D. melanogaster</i>)	w;hs-dCREB2-b 17-2	<i>Yin et al., 1995</i>	FlyBase_ FBti0038019	Gift of Jerry Chi-Ping Yin, University of Wisconsin, Madison

Continued on next page

Continued

Reagent type (species) or resource	Designation	Source or reference	Identifiers	Additional information
Genetic reagent (<i>D. melanogaster</i>)	w[*]; P{w[+mW.hs]=GawB} ey[OK107]/In(4)ci[D], ci[D] pan[ciD] sv[spa-pol] (OK107-Gal4)	Bloomington Stock Center	RRID:BDSC_854	
Genetic reagent (<i>D. melanogaster</i>)	w[*]; P{w[+mC]=UAS-Hsap\KCNJ2.EGFP}7 (UAS-kir2.1)	Bloomington Stock Center	RRID:BDSC_6595	
Genetic reagent (<i>D. melanogaster</i>)	w[*]; P{w[+mC]=Gr21a-GAL4.C} 133t52.1 (Gr21a-Gal4)	Bloomington Stock Center	RRID:BDSC_23890	
Software, algorithm	livetracker	github.com/GershowLab/TrainingChamber (copy archived at URL swh:1:rev:e2a7ccc4e8d845e6cac59d3b2f344cca826c4727 , Lesar, 2021)	This work	

Crosses and genotypes

Larva collection

Flies of the appropriate genotypes (**Table 1**) were placed in 60 mm embryo-collection cages (59–100, Genesee Scientific) and allowed to lay eggs for 6 hr at 25C on enriched food media (Nutri-Fly German Food, Genesee Scientific). For all experiments except otherwise specified, the food was supplemented with 0.1 mM all-trans-retinal (ATR, Sigma Aldrich R2500). Cages were kept in the dark during egg laying. When eggs were not being collected for experiments, flies were kept on plain food at 18C.

Petri dishes containing eggs and larvae were kept at 25C in the dark for 48–60 hr. Second instar larvae were separated from food using 30% sucrose solution and washed in water. Larvae were selected for size. Preparations for experiments were carried out in a dark room.

Y-maze

We used SLA three-dimensional printing to create microfluidic masters for casting (*Karagyozov et al., 2018; Chan et al., 2015*). Masters were designed in Autodesk Inventor and printed on an Ember three-dimensional printer (Autodesk) using black prototyping resin (Colorado Photopolymer Solutions). After printing, masters were washed in isopropyl alcohol, air-dried, and baked at 65C for 45 min to remove volatile additives and non-crosslinked resin. 4% agarose (Apex Quick Dissolve LE Agarose, Cat #20-102QD, Genesee Scientific) was poured over the masters and

Table 1. Crosses used to generate larvae for experiments throughout this work. For strain information, see key resource table.

Figure	Designation	Female parent	Male parent
1	Gr63a ¹	w;Gr63a ¹	
1	OK107>Kir2.1	UAS-Kir2.1-GFP	OK107-Gal4
1	Gr21a>Kir2.1	UAS-Kir2.1-GFP	Gr21a-Gal4
1-4	DANi1>CsChrimson	w;;UAS-CsChrimson	SS00864
1	Driver ctrl		SS00864
1	Effector ctrl	w;;UAS-CsChrimson	
1	58E02>CsChrimson	w;;UAS-CsChrimson	58E02-Gal4
4	hs-dcreb2-b;DANi1>CsChrimson	w;hs-dcreb2-b;UAS-CsChrimson	SS00864

allowed to solidify; then mazes were removed from the mold. Agarose Y-mazes were stored in tap water before use.

The mazes are 1 mm in depth. Each channel is 1.818 mm in length and 0.4 mm in width, and ends in a circular chamber (radius = 1 mm) which redirects larva back to the intersection. An inlet channel (depth = 0.1 mm, length = 1.524 mm, width = 0.1 mm) to the circular chamber connects to tubing for our network of air, CO₂, and vacuum sources.

Behavioral experiments

Individual larvae were selected for size and placed into a Y-maze using a paintbrush. The Y-maze was placed into a PDMS (Sylgard 184, 10:1 base:curing agent) base, where tubing was secured. The Y-maze and base were encased in a dark custom-built box. Larvae were monitored under 850 nm infrared illumination (Everlight Electronics Co Ltd, HIR11-21C/L11/TR8) using a Raspberry Pi NoIR camera (Adafruit, 3100), connected to a Raspberry Pi microcomputer (Raspberry Pi 3 Model B+, Adafruit, 3775). Experiments were recorded using the same camera, operating at 20 fps. Eight copies of the assay were built, to assay the behaviors of multiple larvae in parallel.

Pressure for air, CO₂, and vacuum were controlled at the sources (for vacuum regulation: 41585K43, McMaster-Carr; for pressure regulation: 43275K16, McMaster-Carr). CO₂ and air were humidified through a bubble humidifier. Vacuum, air, and CO₂ tubing to individual assays were separated through a block manifold after pressure control and humidification (BHH2-12, Clippard).

The CO₂ concentration was controlled by a resistive network of tubing connected to the air and CO₂ sources. This inexpensive alternative to a mass-flow controller produced a stable ratio of CO₂ to air that was consistent from day to day and independent of the overall flow rate. The direction of flow was controlled by solenoid pinch valves (NPV2-1C-03-12, Clippard), actuated by a custom circuit we designed.

Custom computer vision software detected the location of the larva in real time. Based on the larva's location, computer controlled valves manipulated the direction of airflow so that the larva was always presented with a fresh set of choices each time it approached the intersection. The software randomly decided which channel would contain air and which contained air mixed with CO₂.

In each maze, one channel was selected to be the outlet for flow and the other two were inlets. An individual larva began in the outlet channel and approached the intersection of the Y-maze, then chose to enter either an inlet branch containing air with CO₂ or an inlet branch containing air only. When the larva's full body entered the chosen channel, software recorded the larva's choice of channel. When the larva reached the end of that channel and entered the circular chamber, valves switched to turn off CO₂ and to switch vacuum to the channel containing larva, making that channel the outlet. The CO₂ remained off (the larva experienced only pure air) until the larva exited the circular chamber. When the larva exited the circular chamber and proceeded towards the intersection, CO₂ was introduced to one randomly selected inlet channel.

Software recorded the location of the larva at every frame (approx 20 Hz); the direction of airflow in the maze (which channel(s) had air; which channel had CO₂ mixed with air, if any; and which channel had vacuum); and all decisions the larva made. We recorded when larvae entered or left a channel, and whether that channel presented CO₂. Larvae could take three actions as they approached the intersection: choose the channel containing air with CO₂ (scored as APPROACH); choose the channel containing pure air (scored as AVOID); or move backwards into their original channel before they reach the intersection. If a larva backed up and reentered the circular chamber it departed from before reaching the intersection, the software reset and presented the larva with a fresh set of choices when it next left the circle. We did not score backing up as a choice of either CO₂ or air.

Following an hour of testing, larvae were trained in the same Y-maze assay used to measure preference. During the training period, unless described otherwise, each 30 s training cycles alternated 15 s of CO₂ presentation, where both inlet channels contained a humidified mix of CO₂ and air; followed by 15 s of air presentation, where both inlet channels had humidified air alone. This cycle was repeated some number of times (specified for each experiment in the figures). Red LEDs (Sun LD, XZM2ACR55W-3) integrated into the setup were used to activate CsChrimson synchronously with CO₂ presentation (paired) or air presentation (reverse-paired).

The volume of the flow chamber was 11.68 mm³ and the volume of the tubing downstream of the valves is approximately 214 mm³. The flow rate exceeded 560 mm³/s, and the state of the chamber was taken to be the same as the state of valves.

Following training, larvae were tested for one hour in an identical scheme to that previously described for the naive measurement.

After larvae were placed into the Y-maze, larva were left in the maze in the dark for a minimum of 5 min. If a larva was not moving through the maze after 5 min, the larva was replaced before the experiment began. If larvae stopped moving through the maze during the first hour of testing, larvae were removed from the maze before training and results were discarded. This happened infrequently (approximately 5% of experiments).

Protocol for timing dependence experiments

For experiments in *Figure 1D*, reward presentation was offset from CO₂ onset. 30 s training cycles alternated 15 s of CO₂ presentation, where both channels contained a mix of CO₂ and air; followed by 15 s of air presentation, where neither channel had CO₂. Red LEDs are used to activate CsChrimson for 15 s. For some larvae, reward onset occurred 7.5 s after CO₂ presentation; for others, reward onset occurred 7.5 s before CO₂ presentation. For all experiments of this type, larvae were presented with 20 cycles of training.

For experiments in *Figure 1E*, 75-second training cycles alternated 15 s of CO₂ presentation, where both inlet channels contained a mix of CO₂ and air with 60 s of air presentation. For some larvae, reward presentation occurred immediately following CO₂ termination for 15 s. For others, reward presentation occurred 15 s prior to CO₂ onset, and reward presentation was terminated upon CO₂ presentation. For a third group of larvae, we rewarded larvae for 15 s between two CO₂ presentations. In this case, 15 s of CO₂ presentation was followed by 15 s of reward presentation in the absence of CO₂, followed by another 15 s of CO₂ presentation. After the second presentation, there was a 30 s air gap before the cycle repeated. For all experiments of these types, larvae were presented with 20 cycles of training.

Habituation and extinction protocols

For experiments in *Figure 3*, we used either an extinction or habituation protocol during training. For both types, larvae were tested for 1 hr to determine their innate CO₂ preference in the method described above.

For extinction experiments, larvae were trained in the same Y-maze used to measure preference. 30 s training cycles alternate 15 s of CO₂ presentation, where both channels contain a mix of CO₂ and air; followed by 15 s of air presentation, where neither channel had CO₂. Red LEDs were used to activate CsChrimson synchronously with CO₂ presentation. This training cycle was repeated some number of times (specified for each experiment above). Immediately after training, we presented the larva with 18 cycles of repeated CO₂/air exposure (15 s of CO₂ followed by 15 s of air; repeat) with no reward pairing. After these extinction cycles, larva preference for CO₂ was tested for one hour.

Habituation experiments were done exactly as for extinction experiments, except that the 18 unrewarded cycles of repeated CO₂/air exposure were presented immediately prior to the training cycles.

For experiments in *Figure 4B*, we tested each larva's initial preference for one hour, then presented three rewarded paired training cycles. For some larvae ('Extinction Post-Train'), we then immediately presented 18 extinction cycles, removed the larvae to food overnight as described above, and then tested their preferences for one hour the next day. For another set of larvae ('Extinction Pre-Test'), we removed the larvae to food immediately following training. The next day, after the larvae were cleaned and inserted into the Y-maze, they were exposed to 18 extinction cycles immediately prior to testing their CO₂ preferences for 1 hr.

Overnight memory formation

For the memory retention experiments of *Figure 4*, testing and training followed identical procedures as above to establish larva preference. After the second round of testing, the larvae were removed from the Y-maze assay with a paintbrush and transferred to an individual 4% agar plate (30 mm, FB0875711YZ Fisher Scientific), with yeast paste added. Larvae were kept in the dark at 18 C for approximately 20 hr. Prior to experiments the next day, larva were removed from the agar plate and washed in water before being placed in a new Y-maze. Larvae were then tested for

CO₂ preference for one hour as previously described. In all experiments in which larvae were removed from the apparatus and later retested, they were placed in the same apparatus but with a new agar Y-maze. Out of 443 larvae placed on agar plates to be tested the following day, 439 larvae were recovered and retested. The four lost larvae were excluded from analysis.

Cycloheximide feeding protocol

For specified experiments in section [Figure 4](#), larva were raised on ATR- food plates at 25°C for 48 hr. Second instar larvae were separated from food using 30% sucrose solution and washed in water. Four hours prior to experiments, larvae were transferred to an agar dish with yeast paste for feeding. Yeast paste was made with either a solution of 35 mM cycloheximide (CXM, Sigma Aldrich C7698) and 0.1 mM all-trans-retinal (ATR, Sigma Aldrich R2500) in 5% sucrose (ATR+/CXM+); or 0.1 mM ATR in 5% sucrose (ATR+/CXM-). To verify CXM ingestion, we placed ATR+/CXM+ and ATR+/CXM- larvae not selected for experiments back on clean food and allowed them to continue development. 95% of ATR+/CXM- larvae pupated, while only 45% of ATR+/CXM+ larvae pupated. Before the experiment, larvae were transferred to an empty petri dish and washed with tap water before being placed into a maze. Except where noted, the same experimental protocol was followed as for non-CXM overnight memory.

Protocol for cycloheximide experiments

For the CXM experiments in section [Figure 4](#), larvae were trained with either a massed or spaced training protocol. The 20x massed training protocol was as previously described for other experiments in [Figure 4](#).

In the 10x spaced training protocol, larvae were first tested for 1 hr to determine their initial CO₂ preference. They then received two cycles of paired DAN-i1 activation with CO₂ presentation (15 s of CO₂ presentation paired with reward, followed by 15 s of air presentation), followed by 15 min of air presentation. This was then repeated five times (10 activations total). In these experiments, we did not test the larvae immediately following training but instead removed them to food and tested their preferences the next day only.

The 10x massed training protocol was identical to the 10x spaced training protocol, except training consisted of 10 sequential cycles of paired DAN-i1 activation with CO₂ presentation (15 s of CO₂ presentation paired with reward, followed by 15 s of air presentation, repeated 10 times). As in the spaced training experiments, larvae were removed to food immediately following training, and their preferences were tested the next day only.

hs-dCREB2-b heat-shock protocol

Petri dishes with larvae were placed in an oven at 37°C for 30 min. The petri dish was placed in a water bath in the oven and covered to preserve humidity and to ensure ATR+ larvae were kept in the dark. The larvae were then removed to 25°C for a 30 min recovery period before experiments. Experiments began immediately after the recovery period. Larvae were kept in the dark at all times during this protocol.

Larvae were tested for CO₂ preference prior to training, immediately following training, and the next day, after being kept overnight on food without ATR. Some larvae in the spaced training groups were not active immediately following training. In the heat-shocked group, 11 out of 24 larvae made less than five decisions during the immediate test; in the not-heat-shocked group, 6 out of 22 larvae made less than five decisions during the immediate test. For this scheme, larvae were in the Y-maze for longer than previous experiments, as the spaced training protocol is 80 min (compared to approximately 10 min or less for the standard massed training). All larvae were retested the following day, even if the larva did not make many decisions when tested immediately following training. After the overnight rest period, all non-heat-shocked and 20/24 heat-shocked larvae were active in the final test period. Inactive larvae were included in the analysis and in the bootstrapping of error bars, but contributed little to the population measure because of the few decisions made.

Development of initial protocols

There are a number of parameters that can be adjusted in our assay, including the identity and concentration of gas used as a CS, the concentration and timing of ATR feeding, the period, duty cycle, and number of CS and US presentations, and duration of behavioral readouts before and after training. We began with our normal protocol for optogenetic activation ([Gepner et al., 2015](#); [Gepner et al., 2018](#)): eggs were laid on ATR supplemented food, and larvae were raised in the dark. We somewhat arbitrarily chose a 30 s, 50% duty cycle applied for 20 cycles as our standard for paired training presentation; we began with DANi1>CsChrimson based on previous work ([Saumweber et al., 2018](#); [Thum and Gerber, 2019](#); [Schleyer et al., 2020](#); [Weiglein et al., 2019](#); [Eschbach et al., 2020b](#)), and the fact that CsChrimson can be activated via red light without provoking a strong visual response. We then adjusted the CO₂ concentration to maximize the contrast between CO₂ preference before and after training. From this basic platform, we changed as little as possible while manipulating the parameter of interest, for example we maintained the 30 s 50% duty cycle paired training while changing the number of cycles, or we maintained 20 cycles while varying the temporal sequence of CS and US presentation, or we used exactly the same 30 s, 50% duty cycle, 20 cycle paired protocol while changing the driver to RF58E02.

Data analysis

The probability of choosing the CO₂ containing channel was scored for individual larvae and for populations as

$$\text{Prob choose CO}_2 = \frac{\#\text{APPROACH}}{\#\text{APPROACH} + \#\text{AVOID}} \quad (3)$$

The population average was determined by dividing the total number of times any larva in the population chose the CO₂ containing channel by the total number of times any larva chose either channel. In other words, larvae that made more decisions contributed more heavily to the average.

The number of larva and total number of approach and avoid decisions made by larvae for each type of experiment is shown in [Table 2](#). Error bars for ‘probability choose CO₂’ data displays and all significance tests in the figures were generated by bootstrapping.

For each experimental set, we performed the bootstrapping as follows. If there were X larvae from that experiment, we selected X larvae with replacement from that set. Then, from each larvae selected, we selected with replacement from the decisions that larvae had made. For example, if the larvae had made Y ‘approach’ and Z ‘avoid’ decisions, we selected (Y+Z) decisions with replacement from that set to represent the larvae. We then calculated the population average from this generated set of animals. We generated 10,000 numerical replicates using this bootstrapping method. Error bars were the standard deviation of these replicates. Note that in each replicate, the same animals were included in each (e.g. trained and untrained) group.

A p-value $p < x$ indicates that at least x fraction of these replicates ended with the same ranking result (e.g. $p < 0.01$ between trained and untrained would indicate that in at least 9900 out of 10,000 replicates, the trained group had a larger CO₂ preference than the untrained group or vice versa). These p-values are included in the ‘Hierarchical Bootstrap’ column of [Table 3](#).

We also performed a non-hierarchical bootstrap, in which animals were resampled but their decisions were not, preserving any correlations between decisions. In this case, we generated 10,000 numerical replicates by selecting with replacement from that set of larvae; the actual sequence of decisions made by the resampled larvae was then used without further resampling. A p-value $p < x$ indicates that at least x fraction of these replicates ended with the same ranking result. These p-values are included in the ‘Bootstrap Animal Only’ column of [Table 3](#). In [Table 3](#), we also show p-values for the Fisher’s exact test, which treats every decision as independent, and the Mann-Whitney u-test, which treats every larva in each group as a discrete measurement and does not account for differing numbers of decisions made by larvae.

To fit the data in [Figure 2](#) to various models, we used a maximum-likelihood approach. First we grouped the larvae according to the number of cycles (n_c) of training they received. In each group, for each larva we quantified the number of decisions made following training. The number of decisions made by the j^{th} larva that received n_c cycles of training was $n(n_c, j)$ and the fraction of times the

Table 2. Data for experiments in **Figure 1**, **Figure 2**, **Figure 3**, and **Figure 4**.

Larva: number of individual larvae tested for experiment type; # Approach Pre-Train: total number of times all larvae chose the channel containing air with CO₂ prior to training; # Avoid Pre-Train: total number of times all larvae chose the channel containing pure air prior to training; # Approach Post-Train: total number of times all larvae chose the channel containing air with CO₂ after the indicated training scheme; # Avoid Post-Train: total number of times all larvae chose the channel containing pure air after the indicated training scheme; # Approach Next Day: total number of times all larvae chose the channel containing air with CO₂ during testing approximately 20 hr after training; # Avoid Next: total number of times all larvae chose the channel containing pure air during testing approximately 20 hr after training. All tests were 1 hr (for each larva).

Experiment	Genotype	# Larva	# Approach Pre-Train	# Avoid Pre-Train	# Approach Post-Train	# Avoid Post-Train	# Approach Next Day	# Avoid Next Day
Figure 1B								
Gr63a ¹	Gr63a ¹	44	831	745	-	-	-	-
DANi1> CsChrimson, ATR+	DANi1> CsChrimson	159	1714	4978	-	-	-	-
DANi1> CsChrimson, ATR-	DANi1> CsChrimson	16	256	614	-	-	-	-
Figure 1D								
Paired	DANi1> CsChrimson	64	561	1760	936	868	-	-
Offset After	DANi1> CsChrimson	20	288	757	316	305	-	-
Reverse Paired	DANi1> CsChrimson	29	315	1022	154	530	-	-
Offset Before	DANi1> CsChrimson	19	218	512	136	315	-	-
Paired, ATR-	DANi1> CsChrimson	16	256	614	127	307	-	-
No Training	DANi1> CsChrimson	50	578	1599	479	1295	-	-
DAN w/o CO ₂	DANi1> CsChrimson	16	260	597	161	354	-	-
Driver ctrl	SS00864	17	110	289	158	358	-	-
Effector ctrl	UAS-CsChrimson	18	214	516	114	294	-	-
58E02> CsChrimson	58E02> CsChrimson	21	380	912	493	501	-	-
Figure 1E								
DANi1> CsChrimson								
Forward Paired		22	181	496	350	337	-	-
Backwards Paired		18	181	438	124	320	-	-
Btw CO ₂		23	272	652	165	283	-	-
Figure 1F								
DANi1> CsChrimson								
6.5%		19	361	568	319	290	-	-
8%		27	256	567	295	255	-	-
15%		19	170	368	249	233	-	-
18%		64	561	1760	936	868	-	-
Figure 2A								
DANi1> CsChrimson								
0 Cycles		50	578	1599	479	1295	-	-
1 Cycles		35	218	606	317	495	-	-
2 Cycles		87	840	2552	1081	1292	-	-
3 Cycles		31	310	930	686	686	-	-
4 Cycles		32	245	712	493	511	-	-
5 Cycles		63	863	2491	975	993	-	-
10 Cycles		14	100	287	154	144	-	-
20 Cycles		64	561	1760	936	868	-	-
Figure 3B								
DANi1> CsChrimson								
2 Cycles, Training		87	840	2552	1081	1292	-	-
2 Cycles, Habituation + Training		30	385	1127	422	554	-	-

Table 2 continued on next page

Table 2 continued

Experiment	Genotype	# Larva	# Approach Pre-Train	# Avoid Pre-Train	# Approach Post-Train	# Avoid Post-Train	# Approach Next Day	# Avoid Next Day
2 Cycles, Training + Extinction		30	336	946	375	793	-	-
3 Cycles, Training		30	308	924	675	679	-	-
3 Cycles, Habituation + Training		18	222	591	260	294	-	-
3 Cycles, Training + Extinction		26	279	695	195	416	-	-
4 Cycles, Training		30	225	659	490	502	-	-
4 Cycles, Habituation + Training		18	239	701	372	352	-	-
4 Cycles, Training + Extinction		27	384	1074	394	475	-	-
5 Cycles, Training		63	863	2491	975	993	-	-
6 Cycles, Habituation + Training		19	266	758	367	324	-	-
6 Cycles, Training + Extinction		18	253	687	309	317	-	-
10 Cycles, Training		14	100	287	154	144	-	-
10 Cycles, Habituation + Training		30	406	1193	607	503	-	-
10 Cycles, Training + Extinction		30	426	1180	401	386	-	-
Figure 4B	DANi1> CsChrimson							
20x		28	380	1172	509	499	459	409
20x (Only Test Next Day)		14	224	768	-	-	296	250
5x		29	472	1427	488	480	404	461
2x		42	514	1537	594	693	201	548
2x (Only Test Next Day)		22	209	696	-	-	213	283
No Train		20	316	889	187	544	104	337
RP 20x		21	282	905	121	430	109	361
Ext Post-Train		23	181	477	-	-	158	365
Ext Pre-Test		31	417	1002	-	-	385	429
Figure 4C	DANi1> CsChrimson							
M 20x (CXM+/ATR+)		20	110	282	252	237	237	272
M 20x (CXM-/ATR+)		17	159	419	271	236	228	235
S 20x (CXM+/ATR+)		23	191	486	-	-	150	316
S 20x (CXM-/ATR+)		20	197	511	-	-	254	264
M 10x (CXM+/ATR+)		23	136	345	-	-	331	344
M 10x (CXM-/ATR+)		20	175	454	-	-	419	375
Figure 4D	DANi1> hs-dCREB2-b; CsChrimson							
M 10x HS		21	175	434	392	370	253	246
M 10x No HS		22	248	656	367	353	451	490
S 10x HS		24	172	420	68	156	153	339
S 10x No HS		22	294	736	212	184	335	352

Table 3. p-Values for experiments in **Figure 1**, **Figure 2**, **Figure 3**, and **Figure 4**.

P-values for experiments were calculated: Bootstrap - p-values calculated as explained in Materials and methods; Fisher - p-values calculated using Fisher's exact test; U-test - p-values calculated using two-sided Mann–Whitney U test. Unless otherwise noted, p-values are calculated between pre-train and post-train data. A shaded row indicates not all tests reach the same significance level (out of ns, $p < 0.05$, $p < 0.01$, $p < 0.001$).

Experiment	Genotype	Hierarchical Bootstrap	Bootstrap Animal Only	Fisher	U-test
Figure 1B					
Gr63a ¹ /DANi1> CsChrimson, ATR+		<10 ⁻⁴	<10 ⁻⁴	<10 ⁻⁴	<10 ⁻⁴
Gr63a ¹ /DANi1> CsChrimson, ATR-		<10 ⁻⁴	<10 ⁻⁴	<10 ⁻⁴	<10 ⁻⁴
Figure 1D					
Paired	DANi1> CsChrimson	<10 ⁻⁴	<10 ⁻⁴	<10 ⁻⁴	<10 ⁻⁴
Offset After	DANi1> CsChrimson	<10 ⁻⁴	<10 ⁻⁴	<10 ⁻⁴	<10 ⁻⁴
Reverse Paired	DANi1> CsChrimson	0.3429	0.2689	0.6166	0.9379
Offset Before	DANi1> CsChrimson	0.4479	0.4373	0.9479	0.9770
Paired, ATR-	DANi1> CsChrimson	0.4762	0.4315	1.000	0.2658
No Training	DANi1> CsChrimson	0.4066	0.3664	0.7726	0.9835
DAN w/o CO ₂	DANi1> CsChrimson	0.3935	0.3102	0.7173	0.4852
Driver ctrl	SS00864	0.3106	0.0313	0.3411	0.3977
Effector ctrl	UAS-CsChrimson	0.3383	0.2361	0.6336	0.8366
58E02> CsChrimson	58E02> CsChrimson	<10 ⁻⁴	<10 ⁻⁴	<10 ⁻⁴	<10 ⁻⁴
Figure 1C					
	DANi1> CsChrimson				
Forward Paired		<10 ⁻⁴	<10 ⁻⁴	<10 ⁻⁴	<10 ⁻⁴
Backwards Paired		0,3368	0.163	0.6801	0.1939
Btw CO ₂		0.0107	0.0001	0.006543	0.0003257
Figure 1D					
	DANi1> CsChrimson				
6.5%		<10 ⁻⁴	<10 ⁻⁴	<10 ⁻⁴	<10 ⁻⁴
8%		<10 ⁻⁴	<10 ⁻⁴	<10 ⁻⁴	<10 ⁻⁴
15%		<10 ⁻⁴	<10 ⁻⁴	<10 ⁻⁴	<10 ⁻⁴
18%		<10 ⁻⁴	<10 ⁻⁴	<10 ⁻⁴	<10 ⁻⁴
Figure 2A					
	DANi1> CsChrimson				
0 Cycles		0.4132	0.3647	0.7726	0.9835
1 Cycles		0.0003	<10 ⁻⁴	<10 ⁻⁴	0.0591
2 Cycles		<10 ⁻⁴	<10 ⁻⁴	<10 ⁻⁴	<10 ⁻⁴
3 Cycles		<10 ⁻⁴	<10 ⁻⁴	<10 ⁻⁴	<10 ⁻⁴
4 Cycles		<10 ⁻⁴	<10 ⁻⁴	<10 ⁻⁴	<10 ⁻⁴
5 Cycles		<10 ⁻⁴	<10 ⁻⁴	<10 ⁻⁴	<10 ⁻⁴
10 Cycles		<10 ⁻⁴	<10 ⁻⁴	<10 ⁻⁴	<10 ⁻⁴
20 Cycles		<10 ⁻⁴	<10 ⁻⁴	<10 ⁻⁴	<10 ⁻⁴
Figure 3B					
	DANi1> CsChrimson				
2 Cycles, Training		<10 ⁻⁴	<10 ⁻⁴	<10 ⁻⁴	<10 ⁻⁴
2 Cycles, Habituation + Training		<10 ⁻⁴	<10 ⁻⁴	<10 ⁻⁴	<10 ⁻⁴
2 Cycles, Training + Extinction		0.0117	0.0020	0.001339	0.04743
3 Cycles, Training		<10 ⁻⁴	<10 ⁻⁴	<10 ⁻⁴	<10 ⁻⁴
3 Cycles, Habituation + Training		<10 ⁻⁴	<10 ⁻⁴	0.0007459	<10 ⁻⁴
3 Cycles, Training + Extinction		0.1133	0.0176	0.1763	0.03069
4 Cycles, Training		<10 ⁻⁴	<10 ⁻⁴	<10 ⁻⁴	<10 ⁻⁴

Table 3 continued on next page

Table 3 continued

Experiment	Genotype	Hierarchical Bootstrap	Bootstrap Animal Only	Fisher	U-test
4 Cycles, Habituation + Training		<10 ⁻⁴	<10 ⁻⁴	<10 ⁻⁴	<10 ⁻⁴
4 Cycles, Training + Extinction		<10 ⁻⁴	<10 ⁻⁴	<10 ⁻⁴	<10 ⁻⁴
5 Cycles, Training		<10 ⁻⁴	<10 ⁻⁴	<10 ⁻⁴	<10 ⁻⁴
6 Cycles, Habituation + Training		<10 ⁻⁴	<10 ⁻⁴	<10 ⁻⁴	<10 ⁻⁴
6 Cycles, Training + Extinction		<10 ⁻⁴	<10 ⁻⁴	<10 ⁻⁴	<10 ⁻⁴
10 Cycles, Training		<10 ⁻⁴	<10 ⁻⁴	<10 ⁻⁴	<10 ⁻⁴
10 Cycles, Habituation + Training		<10 ⁻⁴	<10 ⁻⁴	<10 ⁻⁴	<10 ⁻⁴
10 Cycles, Training + Extinction		<10 ⁻⁴	<10 ⁻⁴	<10 ⁻⁴	<10 ⁻⁴
Figure 4B	DANi1> CsChrimson				
20x Pre-Test/Post-Test		<10 ⁻⁴	<10 ⁻⁴	<10 ⁻⁴	<10 ⁻⁴
20x Pre-Test/Next Day		<10 ⁻⁴	<10 ⁻⁴	<10 ⁻⁴	<10 ⁻⁴
20x (Only Test Next Day) Pre-Test/Next Day		<10 ⁻⁴	<10 ⁻⁴	<10 ⁻⁴	<10 ⁻⁴
5x Pre-Test/Post-Test		<10 ⁻⁴	<10 ⁻⁴	<10 ⁻⁴	<10 ⁻⁴
5x Pre-Test/Next Day		<10 ⁻⁴	<10 ⁻⁴	<10 ⁻⁴	<10 ⁻⁴
2x Pre-Test/Post-Test		<10 ⁻⁴	<10 ⁻⁴	<10 ⁻⁴	<10 ⁻⁴
2x Pre-Test/Next Day		0.2086	0.0501	0.3524	0.07216
2x (Only Test Next Day) Pre-Test/Next Day		<10 ⁻⁴	<10 ⁻⁴	<10 ⁻⁴	<10 ⁻⁴
No Train Pre-Test/Post-Test		0.4035	0.3319	0.7893	0.2003
No Train Pre-Test/Next Day		0.1583	0.0530	0.3071	0.8884
RP 20x Pre-Test/Post-Test		0.2677	0.1507	0.4276	0.7396
RP 20x Pre-Test/Next Day		0.4205	0.3481	0.8474	0.3765
Ext Post-Train Pre-Test/Next Day		0.1801	0.0146	0.3315	0.01336
Ext Pre-Test Pre-Test/Next Day		<10 ⁻⁴	<10 ⁻⁴	<10 ⁻⁴	<10 ⁻⁴
Figure 4C	DANi1> CsChrimson				
M 20x (CXM+/ATR+) Pre-Test/Post-Test		<10 ⁻⁴	<10 ⁻⁴	<10 ⁻⁴	<10 ⁻⁴
M 20x (CXM+/ATR+) Pre-Test/Next Day		<10 ⁻⁴	<10 ⁻⁴	<10 ⁻⁴	<10 ⁻⁴
M 20x (CXM-/ATR+) Pre-Test/Post-Test		<10 ⁻⁴	<10 ⁻⁴	<10 ⁻⁴	<10 ⁻⁴
M 20x (CXM-/ATR+) Pre-Test/Next Day		<10 ⁻⁴	<10 ⁻⁴	<10 ⁻⁴	<10 ⁻⁴
S 10x (CXM+/ATR+) Pre-Test/Next Day		0.1099	0.014	0.1671	0.02985
S 10x (CXM-/ATR+) Pre-Test/Next Day		<10 ⁻⁴	<10 ⁻⁴	<10 ⁻⁴	<10 ⁻⁴
M 10x (CXM+/ATR+) Pre-Test/Next Day		<10 ⁻⁴	<10 ⁻⁴	<10 ⁻⁴	<10 ⁻⁴
M 10x (CXM-/ATR+) Pre-Test/Next Day		<10 ⁻⁴	<10 ⁻⁴	<10 ⁻⁴	<10 ⁻⁴
Figure 4D	DANi1> hs-dCREB2-b; CsChrimson				
M 10x, HS Pre-Test/Post-Test		<10 ⁻⁴	<10 ⁻⁴	<10 ⁻⁴	<10 ⁻⁴
M 10x, HS Pre-Test/Next Day		<10 ⁻⁴	<10 ⁻⁴	<10 ⁻⁴	<10 ⁻⁴
M 10x, No HS Pre-Test/Post-Test		<10 ⁻⁴	<10 ⁻⁴	<10 ⁻⁴	<10 ⁻⁴
M 10x, No HS Pre-Test/Next Day		<10 ⁻⁴	<10 ⁻⁴	<10 ⁻⁴	<10 ⁻⁴
S 10x, HS Pre-Test/Post-Test		0.3804	0.2830	0.7310	0.2750
S 10x, HS Pre-Test/Next Day		0.2645	0.08860	0.4650	0.3802
S 10x, No HS Pre-Test/Post-Test		<10 ⁻⁴	<10 ⁻⁴	<10 ⁻⁴	<10 ⁻⁴
S 10x, No HS Pre-Test/Next Day		<10 ⁻⁴	<10 ⁻⁴	<10 ⁻⁴	<10 ⁻⁴

larva chose the CO₂ containing channel was $p(n_c, j)$. Then we sought a set of parameters θ that maximized

$$\sum_{n_c} \sum_j \log P(p(n_c, j) | n(n_c, j), \theta) \tag{4}$$

where P was the model specific-probability function. For instance, for the quantized learning (two-Gaussian shifting fraction) model:

$$P(p(n_c, j) | n(n_c, j), \theta) = f_u(n_c) \mathcal{N}\left(p(n_c, j), \mu_u, \tilde{\sigma} \sqrt{\frac{\mu_u * (1 - \mu_u)}{n(n_c, j)}}\right) + (1 - f_u(n_c)) \mathcal{N}\left(p(n_c, j), \mu_t, \tilde{\sigma} \sqrt{\frac{\mu_t * (1 - \mu_t)}{n(n_c, j)}}\right) \tag{5}$$

where $\mathcal{N}(x, \mu, \sigma) = \frac{1}{\sqrt{2\pi\sigma^2}} \exp -\frac{(x-\mu)^2}{2\sigma^2}$ and the parameters θ are

$$\theta = \{\mu_u, \mu_t, \tilde{\sigma}, f_u(0), f_u(1), f_u(2), f_u(3), f_u(4), f_u(5), f_u(10), f_u(20)\} \tag{6}$$

The parameter $\tilde{\sigma}$ represents an adjustment to the expected variance due to counting statistics. If all larva chose randomly and independently from the two channels with a fixed probability \bar{p} of choosing CO₂, then we would expect that the number of times the CO₂ containing channel would be binomially distributed. For ease of computation, we approximated the binomial distribution as a normal distribution. In this case, the probability density of observing $p(n_c, j)$ given $n(n_c, j)$ would be normally distributed with mean \bar{p} and variance

$$\sigma^2 = \frac{(\bar{p})(1 - \bar{p})}{n(n_c, j)} \tag{7}$$

In fact, we found that after choosing a CO₂ containing channel, both naive and trained larvae are less likely to choose the CO₂ containing channel the next time they approach the intersection. Because the choices are not independent, the variance of the mean of a series of choices is not given by **Equation 7**. Instead, we modeled the variance as

$$\sigma^2 = \tilde{\sigma}^2 \frac{(\bar{p})(1 - \bar{p})}{n(n_c, j)} \tag{8}$$

where $\tilde{\sigma}$ was a global fit parameter in the shifting and exponential fraction models and in the shifting mean model a function of the amount training. This formulation preserves the properties that the variance should increase as the mean probability of choosing CO₂ approaches 50% and should be larger when fewer decisions are averaged together. However, if we instead just assume a single global σ , the results of our analysis (that the exponential fraction model is preferred) are unchanged.

In the graded learning (single Gaussian with shifting mean and variance) model, μ and σ were allowed to change as a function of training. The probability of an individual observation was

$$P(p(n_c, j) | n(n_c, j), \theta) = \mathcal{N}\left(p(n_c, j), \mu(n_c), \frac{\sigma(n_c)}{\sqrt{n(n_c, j)}}\right) \tag{9}$$

and the parameters were

$$\theta = \{\mu(0), \sigma(0), \mu(1), \sigma(1), \mu(2), \sigma(2), \mu(3), \sigma(3), \mu(4), \sigma(4), \mu(5), \sigma(5), \mu(10), \sigma(10), \mu(20), \sigma(20)\} \tag{10}$$

The exponential fraction model is identical to the quantized learning model, except that the fraction of untrained larvae is an exponentially decreasing function of the number of training cycles:

$$f_u(n_c) = \lambda^{n_c} \tag{11}$$

and the parameters were

$$\theta = \{\mu_u, \mu_t, \tilde{\sigma}, \lambda\} \tag{12}$$

These models were then fit to the data by maximizing the log-likelihood of the observed data set using the MATLAB function `fmincon`. The predictions of these fits are shown in **Figure 2**. These results are summarized in **Table 4**, along with the Aikake and Bayes Information Criterion, AIC and BIC, which are used to compare models with different numbers of parameters. According to both AIC and BIC, the exponential fraction model is strongly favored.

Throughout the paper ‘Fraction of larvae trained’ represents the best fit to the two Gaussian shifting fraction model. The error bars represent the uncertainty in the model fit. Specifically, they represent the range of f over which

Table 4. Model fits to data in **Figure 2**.

Shifting Mean and $\tilde{\sigma}$, shifting fraction, and exponential fraction models are presented in **Figure 2**. Model name: name of the model. Formula: expression for the probability of the data given the model and its parameters. # params: number of free parameters in the model. $\Delta \log(P)$ logarithm of the probability of the data given best fit to this model minus logarithm of the probability of the data given the best fit model overall. A higher (less negative) value means the model better fits the data without regard to the number of parameters. ΔAIC , ΔBIC - Aikake and Bayes Information Criterion minus the lowest values over the models tested. Lower numbers indicate model is favored. According to both criterion, the exponential fraction model is strongly favored over the shifting fraction model, and the shifting fraction model is strongly favored over all models except the exponential fractional model.

Model name	Formula	# params	$\Delta \log(P)$	ΔAIC	ΔBIC
Shifting Mean (fixed $\tilde{\sigma}$)	$P \propto \prod_{n_c \in \{0,1,2,3,4,5,10,20\}} \prod_j \mathcal{N}\left(p(n_c, j), \mu(n_c), \tilde{\sigma} \sqrt{\frac{\mu(n_c) * (1 - \mu(n_c))}{n(n_c, j)}}\right)$	9	-42.7	84.86	104.45
Shifting Mean and σ (Graded learning)	$P \propto \prod_{n_c \in \{0,1,2,3,4,5,10,20\}} \prod_j \mathcal{N}\left(p(n_c, j), \mu(n_c), \frac{\sigma(n_c)}{\sqrt{n(n_c, j)}}\right)$	16	-12.9	39.3	86.3
Shifting Fraction (Quantized learning)	$P \propto \prod_{n_c \in \{0,1,2,3,4,5,10,20\}} \prod_j f_u(n_c) \mathcal{N}\left(p(n_c, j), \mu_u, \tilde{\sigma} \sqrt{\frac{\mu_u * (1 - \mu_u)}{n(n_c, j)}}\right) + \dots (1 - f_u(n_c)) \mathcal{N}\left(p(n_c, j), \mu_t, \tilde{\sigma} \sqrt{\frac{\mu_t * (1 - \mu_t)}{n(n_c, j)}}\right)$	11	-3.93	11.3	38.7
Shifting Fraction (3 clusters)	$P \propto \prod_{n_c \in \{0,1,2,3,4,5,10,20\}} \prod_j f_1(n_c) \mathcal{N}\left(p(n_c, j), \mu_1, \tilde{\sigma} \sqrt{\frac{\mu_1 * (1 - \mu_1)}{n(n_c, j)}}\right) + \dots f_2(n_c) \mathcal{N}\left(p(n_c, j), \mu_2, \tilde{\sigma} \sqrt{\frac{\mu_2 * (1 - \mu_2)}{n(n_c, j)}}\right) + \dots (1 - f_1(n_c) - f_2(n_c)) \mathcal{N}\left(p(n_c, j), \mu_3, \tilde{\sigma} \sqrt{\frac{\mu_3 * (1 - \mu_3)}{n(n_c, j)}}\right)$	20	0	21.4	84.1
Exponential Fraction (All-or-none)	$P \propto \prod_{n_c \in \{0,1,2,3,4,5,10,20\}} \prod_j \lambda^{n_c} \mathcal{N}\left(p(n_c, j), \mu_u, \tilde{\sigma} \sqrt{\frac{\mu_u * (1 - \mu_u)}{n(n_c, j)}}\right) + \dots (1 - \lambda^{n_c}) \mathcal{N}\left(p(n_c, j), \mu_t, \tilde{\sigma} \sqrt{\frac{\mu_t * (1 - \mu_t)}{n(n_c, j)}}\right)$	4	-5.3	0	0

Symbol	Definition	Symbol	Definition
n_c	number of training cycles	$p(n_c, j)$	fraction of times j^{th} larva chose CO ₂ after n_c cycles
$\mu(n_c)$	mean probability of choosing CO ₂ after n_c training cycles	$n(n_c, j)$	# choices made by j^{th} larva after n_c training cycles
$\tilde{\sigma}$	global adjustment to binomial standard deviation	$\sigma(n_c)$	training dependent standard deviation
μ_u	probability of larva in untrained group choosing CO ₂	μ_t	probability of larva in trained group choosing CO ₂
$f_u(n_c)$	fraction of larvae in untrained group after n_c cycles	μ_1, μ_2, μ_3	probability of larva in group 1,2,3 choosing CO ₂
$f_1(n_c), f_2(n_c)$	fraction of larvae in groups 1,2 after n_c cycles	λ	fraction of larvae not trained after one cycle
$\mathcal{N}(x, \mu, \sigma)$	normal cdf: $\frac{1}{\sqrt{2\pi\sigma^2}} e^{-\frac{(x-\mu)^2}{2\sigma^2}}$	$\Delta \log(P)$	relative log probability of data given model
AIC	Aikake Information Criterion: $2k - 2 \log(P)$, $k = \#$ params	ΔAIC	AIC - lowest AIC
BIC	Bayes Information Criterion: $k \log(n_A) - 2 \log(P)$, $k = \#$ params, $n_A = \#$ animals	ΔBIC	BIC - lowest BIC

$$\log P(\text{data}|\theta_0, f) \geq \log P(\text{data}|\theta_0, f_0) - \frac{1}{2} \quad (13)$$

where f is the fraction of trained larvae, f_0 , is the best fit fraction of trained larvae, and θ_0 represents the best fit of the remainder of the parameters, which are not adjusted.

Acknowledgements

We thank Jerry Yin for 17–2 hs-dCREB2-b and Marta Zlatić for SS00864. This project was supported by NSF grant 1455015, NIH grant DP2-EB022359, and a Sloan Foundation fellowship to MHG. The funders had no role in the design or analysis of the experiments. The following ORCIDs apply to the authors: 0000-0001-6611-5941 (AL), and 0000-0001-7528-6101 (MG).

Additional information

Funding

Funder	Grant reference number	Author
National Institutes of Health	1DP2EB022359	Amanda Lesar Javan Tahir Jason Wolk Marc Gershow
National Science Foundation	1455015	Amanda Lesar Javan Tahir Jason Wolk Marc Gershow
Alfred P. Sloan Foundation		Marc Gershow

The funders had no role in study design, data collection and interpretation, or the decision to submit the work for publication.

Author contributions

Amanda Lesar, Conceptualization, Data curation, Software, Formal analysis, Investigation, Methodology, Writing - original draft, Writing - review and editing; Javan Tahir, Software; Jason Wolk, Investigation; Marc Gershow, Conceptualization, Formal analysis, Supervision, Funding acquisition, Visualization, Methodology, Writing - original draft, Project administration, Writing - review and editing

Author ORCIDs

Amanda Lesar  <https://orcid.org/0000-0001-6611-5941>

Marc Gershow  <https://orcid.org/0000-0001-7528-6101>

Decision letter and Author response

Decision letter <https://doi.org/10.7554/eLife.70317.sa1>

Author response <https://doi.org/10.7554/eLife.70317.sa2>

Additional files

Supplementary files

- Supplementary file 1. Schematics and production files for y-maze components.
- Transparent reporting form

Data availability

Summary statistics are included as a supplemental table in the article. Animal by animal choices in temporal sequence are provided as supplemental spreadsheets. Video files have been deposited in Dryad.

The following dataset was generated:

Author(s)	Year	Dataset title	Dataset URL	Database and Identifier
Lesar A, Tahir J, Wolk J, Gershow M	2021	Switch-like and persistent learning in individual <i>Drosophila</i> larvae	https://doi.org/10.5061/dryad.hqbzkh1gs	Dryad Digital Repository, 10.5061/dryad.hqbzkh1gs

References

- Aceves-Piña EO, Quinn WG. 1979. Learning in normal and mutant *Drosophila* larvae. *Science* **206**:93–96. DOI: <https://doi.org/10.1126/science.206.4414.93>, PMID: 17812455
- Apostol TM. 1969. *Calculus*. 2nd Edition. Wiley.
- Apostolopoulou AA, Widmann A, Rohwedder A, Pfitzenmaier JE, Thum AS. 2013. Appetitive associative olfactory learning in *Drosophila* larvae. *Journal of Visualized Experiments : JoVE* **1**:4334. DOI: <https://doi.org/10.3791/4334>, PMID: 23438816
- Asahina K, Louis M, Piccinotti S, Vosshall LB. 2009. A circuit supporting concentration-invariant odor perception in *Drosophila*. *Journal of Biology* **8**:9. DOI: <https://doi.org/10.1186/jbiol108>, PMID: 19171076
- Aso Y, Sitaraman D, Ichinose T, Kaun KR, Vogt K, Belliard-Guérin G, Plaçais PY, Robie AA, Yamagata N, Schnaitmann C, Rowell WJ, Johnston RM, Ngo TT, Chen N, Korff W, Nitabach MN, Heberlein U, Preat T, Branson KM, Tanimoto H, et al. 2014. Mushroom body output neurons encode valence and guide memory-based action selection in *Drosophila*. *eLife* **3**:e04580. DOI: <https://doi.org/10.7554/eLife.04580>, PMID: 25535794
- Berck ME, Khandelwal A, Claus L, Hernandez-Nunez L, Si G, Tabone CJ, Li F, Truman JW, Fetter RD, Louis M, Samuel AD, Cardona A. 2016. The wiring diagram of a glomerular olfactory system. *eLife* **5**:e14859. DOI: <https://doi.org/10.7554/eLife.14859>, PMID: 27177418
- Bouzaiane E, Trannoy S, Scheunemann L, Plaçais PY, Preat T. 2015. Two independent mushroom body output circuits retrieve the six discrete components of *Drosophila* aversive memory. *Cell Reports* **11**:1280–1292. DOI: <https://doi.org/10.1016/j.celrep.2015.04.044>, PMID: 25981036
- Buchanan SM, Kain JS, de Bivort BL. 2015. Neuronal control of locomotor handedness in *Drosophila*. *PNAS* **112**:6700–6705. DOI: <https://doi.org/10.1073/pnas.1500804112>, PMID: 25953337
- Busto M, Iyengar B, Campos AR. 1999. Genetic dissection of behavior: modulation of locomotion by light in the *Drosophila melanogaster* larva requires genetically distinct visual system functions. *Journal of Neuroscience* **19**:3337–3344. PMID: 10212293
- Chan HN, Chen Y, Shu Y, Chen Y, Tian Q, Wu H. 2015. Direct, one-step molding of 3D-printed structures for convenient fabrication of truly 3D PDMS microfluidic chips. *Microfluidics and Nanofluidics* **19**:9–18. DOI: <https://doi.org/10.1007/s10404-014-1542-4>
- Das S, Sadanandappa MK, Dervan A, Larkin A, Lee JA, Sudhakaran IP, Priya R, Heidari R, Holohan EE, Pimentel A, Gandhi A, Ito K, Sanyal S, Wang JW, Rodrigues V, Ramaswami M. 2011. Plasticity of local GABAergic interneurons drives olfactory habituation. *PNAS* **108**:E646–E654. DOI: <https://doi.org/10.1073/pnas.1106411108>, PMID: 21795607
- Duffy JB. 2002. GAL4 system in *Drosophila*: a fly geneticist's Swiss army knife. *Genesis* **34**:1–15. DOI: <https://doi.org/10.1002/gene.10150>, PMID: 12324939
- Eichler K, Li F, Litwin-Kumar A, Park Y, Andrade I, Schneider-Mizell CM, Saumweber T, Huser A, Eschbach C, Gerber B, Fetter RD, Truman JW, Priebe CE, Abbott LF, Thum AS, Zlatic M, Cardona A. 2017. The complete connectome of a learning and memory centre in an insect brain. *Nature* **548**:175–182. DOI: <https://doi.org/10.1038/nature23455>, PMID: 28796202
- Eschbach C, Fushiki A, Winding M, Schneider-Mizell CM, Shao M, Arruda R, Eichler K, Valdes-Aleman J, Ohyama T, Thum AS, Gerber B, Fetter RD, Truman JW, Litwin-Kumar A, Cardona A, Zlatic M. 2020a. Recurrent architecture for adaptive regulation of learning in the insect brain. *Nature Neuroscience* **23**:544–555. DOI: <https://doi.org/10.1038/s41593-020-0607-9>, PMID: 32203499
- Eschbach C, Fushiki A, Winding M, Afonso B, Andrade IV, Cocanougher BT, Eichler K, Gepner R, Si G, Valdes-Aleman J, Gershow M, Jefferis GS, Truman JW, Fetter RD, Samuel A, Cardona A, Zlatic M. 2020b. Circuits for integrating learnt and innate valences in the fly brain. *bioRxiv*. DOI: <https://doi.org/10.1101/2020.04.23.058339>
- Eschbach C, Zlatic M. 2020. Useful road maps: studying *Drosophila* larva's central nervous system with the help of connectomics. *Current Opinion in Neurobiology* **65**:129–137. DOI: <https://doi.org/10.1016/j.conb.2020.09.008>, PMID: 33242722
- Eschment M, Franz HR, Güllü N, Hölscher LG, Huh KE, Widmann A. 2020. Insulin signaling represents a gating mechanism between different memory phases in *Drosophila* larvae. *PLOS Genetics* **16**:e1009064. DOI: <https://doi.org/10.1371/journal.pgen.1009064>, PMID: 33104728

- Faucher C**, Forstreuter M, Hilker M, de Bruyne M, M. dB. 2006. Behavioral responses of *Drosophila* to biogenic levels of carbon dioxide depend on life-stage, sex and olfactory context. *The Journal of Experimental Biology* **209**:2739–2748. DOI: <https://doi.org/10.1242/jeb.02297>, PMID: 16809465
- Felsenberg J**, Barnstedt O, Cognigni P, Lin S, Waddell S. 2017. Re-evaluation of learned information in *Drosophila*. *Nature* **544**:240–244. DOI: <https://doi.org/10.1038/nature21716>, PMID: 28379939
- Felsenberg J**, Jacob PF, Walker T, Barnstedt O, Edmondson-Stait AJ, Pleijzier MW, Otto N, Schlegel P, Sharifi N, Perisse E, Smith CS, Lauritzen JS, Costa M, Jefferis G, Bock DD, Waddell S. 2018. Integration of Parallel Opposing Memories Underlies Memory Extinction. *Cell* **175**:709–722. DOI: <https://doi.org/10.1016/j.cell.2018.08.021>, PMID: 30245010
- Fishilevich E**, Domingos AI, Asahina K, Naef F, Vosshall LB, Louis M. 2005. Chemotaxis behavior mediated by single larval olfactory neurons in *Drosophila*. *Current Biology* **15**:2086–2096. DOI: <https://doi.org/10.1016/j.cub.2005.11.016>, PMID: 16332533
- Gallistel CR**, Fairhurst S, Balsam P. 2004. The learning curve: implications of a quantitative analysis. *PNAS* **101**:13124–13131. DOI: <https://doi.org/10.1073/pnas.0404965101>, PMID: 15331782
- Gepner R**, Mihovilovic Skanata M, Bernat NM, Kaplow M, Gershow M. 2015. Computations underlying *Drosophila* photo-taxis, odor-taxis, and multi-sensory integration. *eLife* **4**:e06229. DOI: <https://doi.org/10.7554/eLife.06229>
- Gepner R**, Wolk J, Wadekar DS, Dvali S, Gershow M. 2018. Variance adaptation in navigational decision making. *eLife* **7**:e37945. DOI: <https://doi.org/10.7554/eLife.37945>, PMID: 30480547
- Gerber B**, Biernacki R, Thum J. 2013. Odor-taste learning assays in *Drosophila* larvae. *Cold Spring Harbor Protocols* **2013**:pdb.prot071639. DOI: <https://doi.org/10.1101/pdb.prot071639>, PMID: 23457337
- Gerber B**, Stocker RF. 2007. The *Drosophila* larva as a model for studying chemosensation and chemosensory learning: a review. *Chemical Senses* **32**:65–89. DOI: <https://doi.org/10.1093/chemse/bjl030>, PMID: 17071942
- Gershow M**, Berck M, Mathew D, Luo L, Kane EA, Carlson JR, Samuel AD. 2012. Controlling airborne cues to study small animal navigation. *Nature Methods* **9**:290–296. DOI: <https://doi.org/10.1038/nmeth.1853>, PMID: 22245808
- Gomez-Marin A**, Stephens GJ, Louis M. 2011. Active sampling and decision making in *Drosophila* chemotaxis. *Nature Communications* **2**:441. DOI: <https://doi.org/10.1038/ncomms1455>, PMID: 21863008
- Gomez-Marin A**, Louis M. 2014. Multilevel control of run orientation in *Drosophila* larval chemotaxis. *Frontiers in Behavioral Neuroscience* **8**:38. DOI: <https://doi.org/10.3389/fnbeh.2014.00038>, PMID: 24592220
- He L**, Gulyanov S, Mihovilovic Skanata M, Karagoyozov D, Heckscher ES, Krieg M, Tsechpenakis G, Gershow M, Tracey WD. 2019. Direction selectivity in *Drosophila* proprioceptors requires the mechanosensory channel tmc. *Current Biology* **29**:945–956. DOI: <https://doi.org/10.1016/j.cub.2019.02.025>, PMID: 30853433
- Heckscher ES**, Lockery SR, Doe CQ. 2012. Characterization of *Drosophila* larval crawling at the level of organism, segment, and somatic body wall musculature. *Journal of Neuroscience* **32**:12460–12471. DOI: <https://doi.org/10.1523/JNEUROSCI.0222-12.2012>, PMID: 22956837
- Hige T**, Aso Y, Modi MN, Rubin GM, Turner GC. 2015. Heterosynaptic Plasticity Underlies Aversive Olfactory Learning in *Drosophila*. *Neuron* **88**:985–998. DOI: <https://doi.org/10.1016/j.neuron.2015.11.003>, PMID: 26637800
- Honegger KS**, Smith MA, Churgin MA, Turner GC, de Bivort BL. 2020. Idiosyncratic neural coding and neuromodulation of olfactory individuality in *Drosophila*. *PNAS* **117**:23292–23297. DOI: <https://doi.org/10.1073/pnas.1901623116>, PMID: 31455738
- Honjo K**, Furukubo-Tokunaga K. 2005. Induction of cAMP response element-binding protein-dependent medium-term memory by appetitive gustatory reinforcement in *Drosophila* larvae. *Journal of Neuroscience* **25**:7905–7913. DOI: <https://doi.org/10.1523/JNEUROSCI.2135-05.2005>, PMID: 16135747
- Honjo K**, Furukubo-Tokunaga K. 2009. Distinctive neuronal networks and biochemical pathways for appetitive and aversive memory in *Drosophila* larvae. *Journal of Neuroscience* **29**:852–862. DOI: <https://doi.org/10.1523/JNEUROSCI.1315-08.2009>, PMID: 19158309
- Humbert TH**, Bruegger P, Afonso B, Zlatic M, Truman JW, Gershow M, Samuel A, Sprecher SG. 2018. Dedicated photoreceptor pathways in *Drosophila* larvae mediate navigation by processing either spatial or temporal cues. *Nature Communications* **9**:1260. DOI: <https://doi.org/10.1038/s41467-018-03520-5>, PMID: 29593252
- Isabel G**, Pascual A, Preat T. 2004. Exclusive consolidated memory phases in *Drosophila*. *Science* **304**:1024–1027. DOI: <https://doi.org/10.1126/science.1094932>, PMID: 15143285
- Ison MJ**, Quian Quiroga R, Fried I. 2015. Rapid Encoding of New Memories by Individual Neurons in the Human Brain. *Neuron* **87**:220–230. DOI: <https://doi.org/10.1016/j.neuron.2015.06.016>, PMID: 26139375
- Jacob PF**, Waddell S. 2020. Spaced Training Forms Complementary Long-Term Memories of Opposite Valence in *Drosophila*. *Neuron* **106**:977–991. DOI: <https://doi.org/10.1016/j.neuron.2020.03.013>, PMID: 32289250
- Jones WD**, Cayirlioglu P, Kadow IG, Vosshall LB. 2007. Two chemosensory receptors together mediate carbon dioxide detection in *Drosophila*. *Nature* **445**:86–90. DOI: <https://doi.org/10.1038/nature05466>, PMID: 17167414
- Kandel ER**, Dudai Y, Mayford MR. 2014. The molecular and systems biology of memory. *Cell* **157**:163–186. DOI: <https://doi.org/10.1016/j.cell.2014.03.001>, PMID: 24679534
- Kane EA**, Gershow M, Afonso B, Larderet I, Klein M, Carter AR, de Bivort BL, Sprecher SG, Samuel AD. 2013. Sensorimotor structure of *Drosophila* larva phototaxis. *PNAS* **110**:E3868–E3877. DOI: <https://doi.org/10.1073/pnas.1215295110>, PMID: 24043822

- Karagoyozov D**, Mihovilovic Skanata M, Lesar A, Gershow M. 2018. Recording neural activity in unrestrained animals with Three-Dimensional tracking Two-Photon microscopy. *Cell Reports* **25**:1371–1383. DOI: <https://doi.org/10.1016/j.celrep.2018.10.013>, PMID: 30380425
- Khurana S**, Abu Baker MB, Siddiqi O. 2009. Odour avoidance learning in the larva of *Drosophila melanogaster*. *Journal of Biosciences* **34**:621–631. DOI: <https://doi.org/10.1007/s12038-009-0080-9>, PMID: 19920347
- Klein M**, Afonso B, Vonner AJ, Hernandez-Nunez L, Berck M, Tabone CJ, Kane EA, Pieribone VA, Nitabach MN, Cardona A, Zlatic M, Sprecher SG, Gershow M, Garrity PA, Samuel AD. 2015. Sensory determinants of behavioral dynamics in *Drosophila* thermotaxis. *PNAS* **112**:E220–E229. DOI: <https://doi.org/10.1073/pnas.1416212112>, PMID: 25550513
- Kwon JY**, Dahanukar A, Weiss LA, Carlson JR. 2007. The molecular basis of CO2 reception in *Drosophila*. *PNAS* **104**:3574–3578. DOI: <https://doi.org/10.1073/pnas.0700079104>, PMID: 17360684
- Larkin A**, Karak S, Priya R, Das A, Ayyub C, Ito K, Rodrigues V, Ramaswami M. 2010. Central synaptic mechanisms underlie short-term olfactory habituation in *Drosophila* larvae. *Learning & Memory* **17**:645–653. DOI: <https://doi.org/10.1101/lm.1839010>, PMID: 21106688
- Lesar A**. 2021. TrainingChamber. *Software Heritage*. swh:1:rev:e2a7ccc4e8d845e6cac59d3b2f344cca826c4727. <https://archive.softwareheritage.org/swh:1:dir:b07e905a53e3bd66a5ddd04b1f7156cdc25efd5e;origin=https://github.com/GershowLab/TrainingChamber;visit=swh:1:snp:1cac126d292328c5860ae67dc14254158c4fbae;anchor=swh:1:rev:e2a7ccc4e8d845e6cac59d3b2f344cca826c4727>
- Li HH**, Kroll JR, Lennox SM, Ogundeyi O, Jeter J, Depasquale G, Truman JW. 2014. A GAL4 driver resource for developmental and behavioral studies on the larval CNS of *Drosophila*. *Cell Reports* **8**:897–908. DOI: <https://doi.org/10.1016/j.celrep.2014.06.065>, PMID: 25088417
- Luo L**, Gershow M, Rosenzweig M, Kang K, Fang-Yen C, Garrity PA, Samuel AD. 2010. Navigational decision making in *Drosophila* thermotaxis. *Journal of Neuroscience* **30**:4261–4272. DOI: <https://doi.org/10.1523/JNEUROSCI.4090-09.2010>, PMID: 20335462
- Lyutova R**, Selcho M, Pfeuffer M, Segebarth D, Habenstein J, Rohwedder A, Frantzman F, Wegener C, Thum AS, Pauls D. 2019. Reward signaling in a recurrent circuit of dopaminergic neurons and peptidergic Kenyon cells. *Nature Communications* **10**:3097. DOI: <https://doi.org/10.1038/s41467-019-11092-1>, PMID: 31308381
- Mancini N**, Hranova S, Weber J, Weiglein A, Schleyer M, Weber D, Thum AS, Gerber B. 2019. Reversal learning in *Drosophila* larvae. *Learning & Memory* **26**:424–435. DOI: <https://doi.org/10.1101/lm.049510.119>, PMID: 31615854
- Margulies C**, Tully T, Dubnau J. 2005. Deconstructing memory in *Drosophila*. *Current Biology* **15**:R700–R713. DOI: <https://doi.org/10.1016/j.cub.2005.08.024>, PMID: 16139203
- Neuser K**, Husse J, Stock P, Gerber B. 2005. Appetitive olfactory learning in *Drosophila* larvae: effects of repetition, reward strength, age, gender, assay type and memory span. *Animal Behaviour* **69**:891–898. DOI: <https://doi.org/10.1016/j.anbehav.2004.06.013>
- Owald D**, Felsenberg J, Talbot CB, Das G, Perisse E, Huetteroth W, Waddell S. 2015. Activity of defined mushroom body output neurons underlies learned olfactory behavior in *Drosophila*. *Neuron* **86**:417–427. DOI: <https://doi.org/10.1016/j.neuron.2015.03.025>, PMID: 25864636
- Owald D**, Waddell S. 2015. Olfactory learning skews mushroom body output pathways to steer behavioral choice in *Drosophila*. *Current Opinion in Neurobiology* **35**:178–184. DOI: <https://doi.org/10.1016/j.conb.2015.10.002>, PMID: 26496148
- Pavlov IP**. 1927. *Conditioned Reflexes: An Investigation of the Physiological Activity of the Cerebral Cortex*. Oxford, England: Oxford University Press.
- Perazzona B**, Isabel G, Preat T, Davis RL. 2004. The role of cAMP response element-binding protein in *Drosophila* long-term memory. *Journal of Neuroscience* **24**:8823–8828. DOI: <https://doi.org/10.1523/JNEUROSCI.4542-03.2004>, PMID: 15470148
- Perisse E**, Yin Y, Lin AC, Lin S, Huetteroth W, Waddell S. 2013. Different kenyon cell populations drive learned approach and avoidance in *Drosophila*. *Neuron* **79**:945–956. DOI: <https://doi.org/10.1016/j.neuron.2013.07.045>, PMID: 24012007
- Quinn WG**, Harris WA, Benzer S. 1974. Conditioned behavior in *Drosophila melanogaster*. *PNAS* **71**:708–712. DOI: <https://doi.org/10.1073/pnas.71.3.708>, PMID: 4207071
- Quinn WG**, Dudai Y. 1976. Memory phases in *Drosophila*. *Nature* **262**:576–577. DOI: <https://doi.org/10.1038/262576a0>, PMID: 822344
- Ren Q**, Li H, Wu Y, Ren J, Guo A. 2012. A GABAergic inhibitory neural circuit regulates visual reversal learning in *Drosophila*. *Journal of Neuroscience* **32**:11524–11538. DOI: <https://doi.org/10.1523/JNEUROSCI.0827-12.2012>, PMID: 22915099
- Roediger HL**, Arnold KM. 2012. The one-trial learning controversy and its aftermath: remembering Rock (1957). *The American Journal of Psychology* **125**:127–143. DOI: <https://doi.org/10.5406/amerjpsyc.125.2.0127>, PMID: 22774677
- Rohwedder A**, Wenz NL, Stehle B, Huser A, Yamagata N, Zlatic M, Truman JW, Tanimoto H, Saumweber T, Gerber B, Thum AS. 2016. Four individually identified paired dopamine neurons signal reward in larval *Drosophila*. *Current Biology* **26**:661–669. DOI: <https://doi.org/10.1016/j.cub.2016.01.012>, PMID: 26877086
- Saumweber T**, Rohwedder A, Schleyer M, Eichler K, Chen YC, Aso Y, Cardona A, Eschbach C, Kobler O, Voigt A, Durairaja A, Mancini N, Zlatic M, Truman JW, Thum AS, Gerber B. 2018. Functional architecture of reward learning in mushroom body extrinsic neurons of larval *Drosophila*. *Nature Communications* **9**:1104. DOI: <https://doi.org/10.1038/s41467-018-03130-1>, PMID: 29549237

- Sawin EP**, Harris LR, Campos AR, Sokolowski MB. 1994. Sensorimotor transformation from light reception to phototactic behavior in *Drosophila* larvae (Diptera: drosophilidae). *Journal of Insect Behavior* **7**:553–567. DOI: <https://doi.org/10.1007/BF02025449>
- Scherer S**, Stocker RF, Gerber B. 2003. Olfactory learning in individually assayed *Drosophila* larvae. *Learning & Memory* **10**:217–225. DOI: <https://doi.org/10.1101/lm.57903>, PMID: 12773586
- Schleyer M**, Fendt M, Schuller S, Gerber B. 2018. Associative learning of stimuli paired and unpaired with reinforcement: evaluating evidence from maggots, flies, bees, and rats. *Frontiers in Psychology* **9**:1494. DOI: <https://doi.org/10.3389/fpsyg.2018.01494>, PMID: 30197613
- Schleyer M**, Weiglein A, Thoener J, Strauch M, Hartenstein V, Kantar Weigelt M, Schuller S, Saumweber T, Eichler K, Rohwedder A, Merhof D, Zlatic M, Thum AS, Gerber B. 2020. Identification of Dopaminergic Neurons That Can Both Establish Associative Memory and Acutely Terminate Its Behavioral Expression. *Journal of Neuroscience* **40**:5990–6006. DOI: <https://doi.org/10.1523/JNEUROSCI.0290-20.2020>, PMID: 32586949
- Schwaerzel M**, Heisenberg M, Zars T. 2002. Extinction antagonizes olfactory memory at the subcellular level. *Neuron* **35**:951–960. DOI: [https://doi.org/10.1016/s0896-6273\(02\)00832-2](https://doi.org/10.1016/s0896-6273(02)00832-2), PMID: 12372288
- Smith M**, Honegger KS, Turner G. 2021. Idiosyncratic learning performance in flies generalizes across modalities. *bioRxiv*. DOI: <https://doi.org/10.1101/2021.01.23.427920>
- Sun X**, Heckscher ES. 2016. Using Linear Agarose Channels to Study *Drosophila* Larval Crawling Behavior. *Journal of Visualized Experiments* **117**:e54892. DOI: <https://doi.org/10.3791/54892>, PMID: 27929468
- Takemura SY**, Aso Y, Hige T, Wong A, Lu Z, Xu CS, Rivlin PK, Hess H, Zhao T, Parag T, Berg S, Huang G, Katz W, Olbris DJ, Plaza S, Umayam L, Aniceto R, Chang LA, Lauchie S, Ogundeyi O, et al. 2017. A connectome of a learning and memory center in the adult *Drosophila* brain. *eLife* **6**:e26975. DOI: <https://doi.org/10.7554/eLife.26975>, PMID: 28718765
- Thum AS**, Gerber B. 2019. Connectomics and function of a memory network: the mushroom body of larval *Drosophila*. *Current Opinion in Neurobiology* **54**:146–154. DOI: <https://doi.org/10.1016/j.conb.2018.10.007>, PMID: 30368037
- Tully T**, Boynton S, Brandes C, Dura JM, Mihalek R, Preat T, Vilella A. 1990. Genetic dissection of memory formation in *Drosophila melanogaster*. Cold Spring Harbor Symposia on Quantitative Biology 203–211.
- Tully T**, Preat T, Boynton SC, Del Vecchio M. 1994. Genetic dissection of consolidated memory in *Drosophila*. *Cell* **79**:35–47. DOI: [https://doi.org/10.1016/0092-8674\(94\)90398-0](https://doi.org/10.1016/0092-8674(94)90398-0), PMID: 7923375
- Twick I**, Lee JA, Ramaswami M. 2014. Olfactory habituation in *Drosophila*-odor encoding and its plasticity in the antennal lobe. *Progress in Brain Research* **208**:3–38. DOI: <https://doi.org/10.1016/B978-0-444-63350-7.00001-2>, PMID: 24767477
- Vaadia RD**, Li W, Voleti V, Singhanian A, Hillman EMC, Grueber WB. 2019. Characterization of Proprioceptive System Dynamics in Behaving *Drosophila* Larvae Using High-Speed Volumetric Microscopy. *Current Biology* **29**:935–944. DOI: <https://doi.org/10.1016/j.cub.2019.01.060>, PMID: 30853438
- Vogt K**, Yarali A, Tanimoto H. 2015. Reversing Stimulus Timing in Visual Conditioning Leads to Memories with Opposite Valence in *Drosophila*. *PLOS ONE* **10**:e0139797. DOI: <https://doi.org/10.1371/journal.pone.0139797>, PMID: 26430885
- Weiglein A**, Gerstner F, Mancini N, Schleyer M, Gerber B. 2019. One-trial learning in larval *Drosophila*. *Learning & Memory* **26**:109–120. DOI: <https://doi.org/10.1101/lm.049106.118>, PMID: 30898973
- Werkhoven Z**, Rohrsen C, Qin C, Brembs B, de Bivort B. 2019. MARGO (Massively Automated Real-time GUI for Object-tracking), a platform for high-throughput ethology. *PLOS ONE* **14**:e0224243. DOI: <https://doi.org/10.1371/journal.pone.0224243>, PMID: 31765421
- Widmann A**, Artinger M, Biesinger L, Boepple K, Peters C, Schlechter J, Selcho M, Thum AS. 2016. Genetic Dissection of Aversive Associative Olfactory Learning and Memory in *Drosophila* Larvae. *PLOS Genetics* **12**:e1006378. DOI: <https://doi.org/10.1371/journal.pgen.1006378>, PMID: 27768692
- Widmann A**, Eichler K, Selcho M, Thum AS, Pauls D. 2018. Odor-taste learning in *Drosophila* larvae. *Journal of Insect Physiology* **106**:47–54. DOI: <https://doi.org/10.1016/j.jinsphys.2017.08.004>, PMID: 28823531
- Wu Y**, Ren Q, Li H, Guo A. 2012. The GABAergic anterior paired lateral neurons facilitate olfactory reversal learning in *Drosophila*. *Learning & Memory* **19**:478–486. DOI: <https://doi.org/10.1101/lm.025726.112>, PMID: 22988290
- Wu JK**, Tai CY, Feng KL, Chen SL, Chen CC, Chiang AS. 2017. Long-term memory requires sequential protein synthesis in three subsets of mushroom body output neurons in *Drosophila*. *Scientific Reports* **7**:7112. DOI: <https://doi.org/10.1038/s41598-017-07600-2>, PMID: 28769066
- Yin JC**, Wallach JS, Del Vecchio M, Wilder EL, Zhou H, Quinn WG, Tully T. 1994. Induction of a dominant negative CREB transgene specifically blocks long-term memory in *Drosophila*. *Cell* **79**:49–58. DOI: [https://doi.org/10.1016/0092-8674\(94\)90399-9](https://doi.org/10.1016/0092-8674(94)90399-9), PMID: 7923376
- Yin JC**, Del Vecchio M, Zhou H, Tully T. 1995. CREB as a memory modulator: induced expression of a dCREB2 activator isoform enhances long-term memory in *Drosophila*. *Cell* **81**:107–115. DOI: [https://doi.org/10.1016/0092-8674\(95\)90375-5](https://doi.org/10.1016/0092-8674(95)90375-5), PMID: 7720066
- Yu D**, Akalal DB, Davis RL. 2006. *Drosophila* alpha/beta mushroom body neurons form a branch-specific, long-term cellular memory trace after spaced olfactory conditioning. *Neuron* **52**:845–855. DOI: <https://doi.org/10.1016/j.neuron.2006.10.030>, PMID: 17145505